DRAFT - Do not Cite or Quote

Consequences Analysis of Using ISC-PRIME Over the Industrial Source Complex Short Term Model

Staff Report

U.S. Environmental Protection Agency
Office of Air Quality Planning and Standards
Emissions, Monitoring, and Analysis Division
Research Triangle Park, NC 27709

April 1998

DISCLAIMER

This draft report has not been reviewed by The Office of Air Quality Planning and Standards, U.S. Environmental Protection Agency, and has not been approved for publication. Mention of trade names or commercial products is not intended to constitute endorsement or recommendation for use.

PREFACE

Before a new algorithm or model is released for use by the air quality modeling community, there is a need to understand how that algorithm or model will affect concentration results with respect to measured observations. The incorporation of the Plume Rise Model Enhancements (PRIME) model into the Industrial Source Complex Short Term (ISCST3) model to form ISC-PRIME is a major alteration of the way in which building downwash is calculated. An independent evaluation has been performed in which the concentration output from ISCST3 and ISC-PRIME have been compared with measured observations from three field studies and one wind tunnel study. Herein is a review of that evaluation, review of a subsequent independent consequences analysis, and further analysis of data results.

Contents

FIGURES

Tables

1. INTRODUCTION

Deficiencies in the current Building Downwash algorithms are well known. These deficiencies include: 1) reported over predictions under light wind, stable conditions, 2) discontinuities in the vertical, alongwind, and crosswind directions, and 3) the assumption that the source is always collocated with the structure causing down washing.

To address these deficiencies, the Electric Power Research Institute (EPRI) funded evaluations of a series of field and wind tunnel experiments from which a new downwash algorithm was derived and called PRIME, Plume Rise Model Enhancements. The PRIME algorithm was developed, codified, and incorporated into the Industrial Source Complex Short Term model (ISCST3) by Earth Tech, Inc. The PRIME modified modeled was named ISC-PRIME. Independent evaluations of ISC-PRIME were conducted and draft documents were prepared by ENSR, under contract to EPRI. EPRI presented the U.S. EPA with the ISC-PRIME software, together with the results of independent evaluation and consequences analysis.

EPA has conducted its own Consequences Analysis (CA) of the ISC-PRIME software and a review of the EPRI independent reports. The analysis consists of verifying the ENSR CA results, verifying that ISCST3 and ISC-PRIME produce the same results with no building in the input, an analysis of BPIP as modified for use in preparing input for ISC-PRIME, and an analysis of the consequences of using ISC-PRIME instead of ISCST3 for building downwash situations.

2. TECHNICAL DESCRIPTION

The current ISCST3 model contains two downwash algorithms, the Huber-Snyder and Schulman-Scire algorithms. The Huber-Snyder algorithm applies to stacks that are lower than building height (BH) plus 1.5 times the lesser of building height or projected building width (L). The Schulman-Scire algorithm supersedes the Huber-Snyder algorithm when stack heights are less than or equal to BH + 0.5L. Activation of either algorithm is dependent upon the wake effect height at 2 BH's downwind to be less than or equal to BH + 2L or BH + 1.5L, respectively. These algorithms have limitations: 1) the stack is assumed to be located in the center of the lee wall of the structure causing down washing even though it may be upwind, far downwind, or laterally displaced from the structure, 2) there are discontinuities between the wake and non wake areas, 3) streamline flow over a structure is not taken into account, 4) plume rise is not adjusted due to the velocity deficit in the wake or due to vertical wind speed shear, 5) concentrations in the cavity region are not linked to material capture, and 6) under light wind speed, stable conditions, concentration estimates are reported to be higher than observed.

To address these issues, the PRIME model was created and incorporates two fundamental features: enhanced plume dispersion coefficients due to the wake turbulence, and reduced plume rise caused by descending streamlines and increased entrainment in the wake of a structure. The PRIME model was integrated into ISCST3 (dated 96113) and named ISC-PRIME (dated 97224).

The foundation of the PRIME model is its ability to model the downwind cavity (near wake) and far wake areas on a three-dimensional scale. The dimensions of the downwashing structure are used to form an ellipsoidal shape that may consist of a rooftop and downwind cavity, or a single recirculation cavity (Figure 1). The recirculation cavity is defined as the region bounded above the roof by the separation streamline formed at the upwind roof edge and bounded downwind by the reattachment streamline. The lateral sides of the structure form the side of the ellipsoidal cavity (Figure 2).

Upon the cavity "foundation," streamlines are formed based on the location and maximum height of the rooftop recirculation cavity, the length of the downwind recirculation cavity and the building length scale. Upwind streamlines ascent to the point of the maximum rooftop recirculation cavity height and descend thereafter. There is a gradual decrease in the rate of streamline descent in the far wake region.

The plume rise component of PRIME is computed using a numerical solution of the mass, energy, and momentum conservation laws. The model permits arbitrary ambient temperature stratification, unidirectional wind sheer and an initial plume size. Streamline ascent and decent effects on plume rise are considered as well as the enhanced dilution due to building induced turbulence. Dispersion is based on Weil (1996).

3. ANALYSIS METHOD

This CA is divided into several parts. These parts consist of: 1) confirming that with no building in the input files, both ISCST3 and ISC-PRIME produce the same results, 2) reviewing the ENSR Independent Evaluation and CA, 3) confirming the modeling results of the ENSR independent CA, and 4) performing an additional assessment of ISC-PRIME.

In the first part, the input files consisted of a single source (See Appendix A) with four groups of receptors. The source is a 35-meter height point source with a buoyant plume. There are four 21 by 21 receptor grid arrays with spacings of 50, 200, 500, and 1000 meters covering an area from 1 km up to 10 km square and centered on the source. One year of 1964 Pittsburgh, PA meteorological data was used in all runs. The programs printed the maximum and highest of the second highest 1-, 3-, 24-hour averaged concentrations for all receptors and the annual average for all receptors.

In the second part, the ENSR independent evaluation and the CA reports were reviewed. The ENSR independent evaluation consisted of four data sets:

1. A conventional 1-year monitoring network near the Bowline Point Station, New York (source type: electric utility; two 600MW units, each with an 86.9-m stack; monitor coverage consisted of four close-in sites at distances from 251 to 848 meters.)

2. A tracer experiment conducted by the American Gas Association (AGA) in Texas and Kansas (source type: gas compressor station stacks; 63 hours available; tracer sampler coverage from 50 to 200 meters.)

3. A tracer experiment at the EOCR Test Reactor Building in Idaho (source type: nonbuoyant releases at 30m, 25m and ground level; 22 release hours.)

4. A wind tunnel study of the Lee Power Plant (source type: 64.8m steam boiler stacks; each stack 64.8 meters high; numerous cases studied: in neutral conditions, 78 combinations of wind direction, wind speed, and plume buoyancy; in stable conditions, 14 combinations of wind direction and plume buoyancy; tracer sampler coverage at six distances ranging from 150-900 meters)

In the third part, the ENSR CA was rerun to confirm their results. Five buildings were used as input. The buildings consisted of a Squat 34m and 50m high building of 60m x 120m length and width, a Tall 34m and 50 m high building of 30m square base, and a Super Squat 34m high building of 180m square base (Appendix B). There were two sources 35m and 100m high. These sources were placed on the northeast corner of each building and then again at a distance of four building heights to the northeast of each building. Runs were also conducted using no building at all. 1964 Pittsburgh, PA meteorological data was used for each run. The CA receptor grids are the same ones used in Part 1 of this analysis.

The fourth part consists of scenarios and runs made to ascertain the characteristics and consequences of using ISC-PRIME with respect to ISCST3 using the ENSR CA input data sets. ISCST3 consists of two downwash algorithms, Huber-Snyder, and Schulman-Scire. The ratio of the height of the stack with respect to the lesser of the building height or projected width will cause one or the other algorithm to be used in a downwash situation provided that the plume rise is less than the height of the building plus 2L or 1.5L within two building heights of the source, respectively. The ENSR CA input buildings, stack heights, and buoyancy provided an adequate test of these two algorithms. The Cartesian receptor grid networks were replaced with a 20-ring polar grid network. The binary hourly output files from the EPRI CA runs were reanalyzed for maximum and highest of the second concentrations, on a ring by ring basis, between ISCST3 and ISC-PRIME.

Because of the coding of streamlines into PRIME, there are questions about how multi-tiered buildings should be modeled. Effluents emitted into a streamline can be captured, partially captured, or not captured by a tier's recirculation cavity. This can have a dramatic effect on calculated concentrations. If a stack's effluent is captured in the cavity of one tier and not in the cavity of the highest tier, selection of the proper tier is paramount. BPIP selects the tier with the highest wake effect height which is not always the correct tier for inclusion into ISC-PRIME.

Runs were set up to examine the consequences of using BPIP selected tiers for inclusion in ISC-PRIME runs. A tall tier was placed on top of a squat building and a stack was initially set at the far end. Additional runs involved setting the stack to different heights and moving the stack away from the squat building end. The runs also involve moving the tall tier toward the stack end of the squat building. The purpose was to see how ISC-PRIME would react to tier selection and subsequent concentration calculations. The stack emissions rates were set for an almost neutrally buoyant plume (slight rise). A SCREEN set of meteorological conditions was used and the wind directions were set to upwind and then downwind directions with a line of receptors placed along the longitudinal centerline of the squat building out to 5km.

The stack exit velocity and exit temperature were set to produce a near buoyant plume rise with little momentum. This was done for two reasons. First, this would test the behavior of ISC-PRIME for a small industrial source venting "fumes" to the outside air from the ambient air inside the building. What would the concentrations be in the cavity and just outside the cavity?

Second, this type of low plume rise would allow the exploration of plume transport and dispersion from along various streamlines. The low buoyancy and momentum would allow the plume to reach "final plume rise" quickly and near the targeted streamline. It would also be used to gather data to study the effects of tier selection by BPIPPRM.

4. ANALYSIS RESULTS

4.1 Model Runs Without Buildings

In the first part, ISC-PRIME (dated 97224) was run with the same input data set as ISCST3 (dated 96113) with no building data in the input file. A file comparison showed the only differences to be in the precision of some of the printed values. There were minor differences in the 10,000th decimal place and smaller. There were no major differences in any of the runs. Both models produced the same results.

4.2 Significant Findings of ENSR Independent Evaluation

In the second part, a review of the ENSR independent evaluation's four sets of results was performed. These sets included the Bowline Point ambient monitoring, the AGA and EOGR tracer experiment, and Lee Power Plant wind tunnel results. In the following, the most significant findings of the ENSR evaluation are identified.

Bowline Point Results Analysis

The Bowline Point evaluation results included tables of top 50 monitoring data values from the plant's Bowline Point, Boat Ramp, Met Tower and Parking Lot monitors. These four

monitors are located at distances from 251 to 848 meters from the plant. Three monitors at greater distances from the plant were not included in the evaluation.

The Bowline Point and Boat Ramp monitors recorded the highest and greater number of concentration values than the other two close in monitors. Highest observed concentrations were under stable conditions under moderate (5 to 10 m/s) to high (> 11 m/s) wind speeds. Similar yet conservative concentrations were calculated by both models. However, the highest concentrations calculated by ISCST3 were produced under moderate wind speeds and more stable conditions than those observed under ambient conditions where as the highest concentrations calculated by ISC-PRIME were under high wind speeds and neutral conditions, the same conditions that also produced the highest observed concentrations.

Quantile-quantile figures of modeled vs. observed concentrations, unpaired in time, show both models to be conservative (Figures 3 and 4). ISCST3 tends to be more conservative at the extreme high end of the curve where the results are slightly less conservative with calculated concentrations becoming nonconservative approximately an order of magnitude below the maximum concentration. Otherwise, the ISC-PRIME results are generally more conservative than the ISCST3 values to the point where some of the values are greater than a factor of two. Except as noted, all top 50 concentrations of both models were conservative and the ISC-PRIME model was able to produce those concentrations under conditions matching the ambient conditions producing the highest concentrations.

AGA Results Analysis

This study consisted of two different sites, one in Texas and the other in Kansas. Both buildings, one in each state, were elongated squat and super squat buildings, respectively (Figures 5a and b). The Texas site had a stack that was offset from the building with a stack height that was 85% of the building height of 11.37m. The Kansas site had two offset stacks, one 80% of the building height and the other twice as tall as the building height of 12.19m. A figure of the receptor layout arcs was provided for the Texas site but not the Kansas site. One interesting aspect of the study is that the source appears to be upwind of the building. Also, the source is offset toward a corner where the plume could be effected by the dynamics of wind flow around a building corner. The arcs are at 50, 100, 150, and 200 meters from the source with the arcs being at 5L or more from the building where L is the lesser of the building height or projected width.

The observed concentrations were adjusted using a technique that examines the concentrations at all receptors along an arc and derives an estimate of the Sigma Y and subsequent maximum concentration value using the program PLMFIT by Irwin (1996). The resultant estimates were used as input to a series of scatter and residual plots. A residual plot of the modeled versus observed concentrations versus the four downwind distances showed both ISCST3 and ISC-PRIME to be conservative and ISCST3 to be more conservative than ISC-PRIME (Figure 6). At a distance of 200 meters (approximately 17L) downwind of the buildings,

it is indeterminate as to whether ISCST3 or ISC-PRIME does a better predictive analysis of concentrations.

Using the ISCST3 results, two additional residual plots of wind speed and stability class were generated. The one of the plots shows that there is more scatter in the results as the wind speeds decrease. In the other plot, for the more stable and unstable stability classes, the scatter is greater than for the more neutral and less stable of the stable stability classes (Figure 7). Part of this may be due to the lower number of observations A(2) and E(9) versus B(12), C(35), and D(34) (Figure 8). Still, there is a definite trend.

Two additional plots were also generated using ISC-PRIME results. The wind speed plot shows more scatter in the predicted versus observed ratio as the wind speeds decrease. This is understandable. The other plot showed that even more scatter for stability class E values than ISCST3 and a more conservative plot for stability class A values (Figures 7 and 8). Except for stability class E results, there was less scatter in the ISC-PRIME results. This may also help to explain how stability class A concentrations showed up in the top ISC-PRIME concentrations for the Bowline Point receptor.

EOCR Results Analysis

The EOCR used a two-tier building with the first tier roof at 7m and the second tier roof at 25m above plant grade (Figure 9). Both tiers were square with a common corner on the west side. The shorter tier was super squat and the second tier was tall. There were six rings of receptors at 50, 100, 400, 800, 1200, and 1600 meters from the plant center. As in the AGA study, results were adjusted using PLMFIT.

Residual plots of predicted over observed concentrations versus distance showed both ISCST3 and ISC-PRIME to be conservative overall with almost negligible differences from the 100 meter ring outward (Figure 10). The scatter along the 50 meter ring was less for the ISC-PRIME runs. There was a slight but notable rise in the bias toward more conservative results for both models as the downwind distance increased.

The wind speed residual pattern showed that both models produced conservative results and that ISCST3 was a little more conservative and had a little more data scatter than ISC-PRIME (Figure 11). The same could be said for the stability class residual plot (Figure 12).

Lee Power Plant Wind Tunnel Analysis

A wind tunnel simulation of the Lee Power Plant was performed with six receptor scale distances of 50, 100, 400, 800, 1200, and 1600 meters from the source (Figure 13). Short term sampling averages of 5 minutes were converted to 1-hour averages using the 1/5 power law (Turner, 1969). Stability classes of rural stable and urban neutral were simulated.

Under simulated urban neutral, both models tended to under predict observed concentrations by less than a factor of eight in almost all cases. ISC-PRIME was generally more conservative than ISCST3 except close-in at a simulated distance of 150 meters (figure 14). Under prediction generally occurred at simulated wind speed at or above 20 m/s. The lower the wind speed, the higher the over prediction and the more conservative the modeled results. In the 0-5.6 m/s category, both models over predicted by a factor of 10 or more (Figure 15).

Under simulated rural stable conditions, the ISCST3 modeled results were conservative by between one and two orders of magnitude. The ISC-PRIME results were slightly conservative from 600 meters outward but became quickly non conservative to four orders of magnitude a distance of 150 downwind (Figure 16).

There is support for this in the Bowline point data. Tables 1 and 2 show that ISC-PRIME (and ISCST3) tend to under calculate concentrations at the close in Parking Lot and Met Tower monitor sites.

4.3 Model Runs to Confirm ENSR CA

The ENSR CA runs were duplicated. The EPA duplicated output files were reviewed against the values reported in the ENSR CA. Only minor discrepancies were found and the overall conclusions were not affected.

4.4 EPA Runs using ENSR CA Input Data

The same input data sets used in the ENSR CA were used as input to these runs (Appendix A). The 1964 Pittsburgh, PA meteorological data set was also used. Unless otherwise noted (eg. “No Bldg”), the 35 m stack results were produced with buildings that were 34 meters high while the 100m stack results were produced with buildings that were 50 meters high. With respect to the ISCST3 results, the 35 meter results were produced using the Schulman-Scire algorithm while the 100 meter results were produced using the Huber-Snyder algorithm.

In the “No Bldg” (no building) cases and using the same input for respective runs, the maximum and highest of the second highest 1-, 3-, 24-hour and annual average values for all receptors were the same between respective ISCST3 and ISC-PRIME runs. The ISCST3 and ISC-PRIME results mirrored each other at all respective 20 downwind distances from 50 meters to 10 km. This occurred under urban and rural conditions and at stack heights of 35 and 100 meters.

In the Schulman-Scire 35m stack (34m Squat building) cases, the ISCST3 rural concentrations rise up to maximum peaks above 7500 ug/m^3 at or just before 200 meters from the stacks and then decrease asymtopically whether the stack is on the corner or away from the building. The ISC-PRIME highest values for stacks located on the corner are less than 30% of the ISCST3 values (Figure 17). ISCST3, as well as ISC-PRIME, highest of the second highest

values are very similar to their respective maximum concentrations in all cases. The ISC-PRIME maximum value for a Tall building with the stack located on the corner occurred at 50 meters from the stack and there are indications that the actual maximum may be higher (Figure 18). When the stack is located to the northeast of the building, the ISC-PRIME maximum values are 5% to 10% of the respective ISCST3 maximum values (Figure 19).

Under urban conditions, ISCST3 concentrations rise to a maximum peak above 2500 ug/m^3 and with their highest of the second highest values appearing to coincide with their maximum value counterpart. The ISC-PRIME values are 90% of the ISCTST3 values to 25% greater than their ISCST3 counterparts (Figures 20 and 21). When the stack is moved to the northeast of the buildings, ISC-PRIME concentrations are about a third of the ISCST3 maximum concentrations (Figure 22).

In the Huber-Snyder 100m stack (50m building) cases, the ISCST3 rural concentrations rise up to maximum peaks above 60 ug/m^3 after 400 meters from the stacks. The ISC-PRIME highest values for stacks located on the corner are 20% to 50% greater than their ISCST3 counterparts (Figure 23). ISCST3 and ISC-PRIME highest of the second highest values are close to their respective maximum concentrations in all cases.

Multimodal peaks appear in many of the ISCST3 and ISC-PRIME curves. This occurs whether the stack is on the corner or away from the building. These peaks also appeared in similar plots where no buildings were present in the input.

The ISC-PRIME maximum values for stacks located northeast of the buildings are equal to 20% greater than their ISCST3 counterparts. However, the highest of the second highest ISC-PRIME values are equal to 30% less than their ISCST3 counterparts (Figure 24). This is a significant drop off with respect to possible design concentrations in close to the stack. However, as distances downwind increase, the ISCST3 and ISC-PRIME maximum and highest of the second highest values merge or significantly converge by 10 km downwind with the ISC-PRIME values being at or greater than ISCST3 values. Differences at 2 km are appearent but not overly significant.

Under urban conditions, ISCST3 concentrations rise to a maximum peak of around 100 ug/m^3 and with their highest of the second highest values appearing to be less than their maximum value counterpart. The ISC-PRIME values are 20 to 50% greater than their ISCST3 counterparts (Figure 25). When the stack is moved to the northeast of the buildings, ISC-PRIME concentrations are about 20% greater than their ISCST3 counterparts (Figure 26).

5. CONCLUSIONS

When no building data was included in the input files, the ISC-PRIME model was able to reproduce ISCST3 results for over 1600 receptors, urban and rural settings, two different stack

heights and respective values using one year of hourly meteorological data. The incorporation of the PRIME algorithms into ISCST3 is transparent to users when "no building" input data sets are used and therefore the PRIME algorithms do not interfere with the no downwash functions of the ISCST3 model.

The three field study results showed that ISC-PRIME can be more to less conservative than ISCST3. This is dependent upon the stack-building relationship, downwind distance, windspeed, stability class and emission factors. Overall and at various distances downwind, ISC-PRIME tends to be less conservative than ISCST3, but more conservative than observed values.

The EPA analysis using the ENSR CA input data sets shows that the ENSR CA values can be duplicated and that either model can calculate concentrations that are higher than the other model's concentrations. Given the same input data, the model output differences are dependent upon stack location, stack to building height, urban or rural setting, downwind distance. For all runs, as the downwind distance increases beyond about 1 km, the ISC-PRIME and ISCST3 values converge. After 10 km downwind, the values, in most cases, are practically the same.

The studies so far have dealt with moderate to high stack exit velocities. When low exit velocities and near ambient temperatures were used to generate slightly buoyant low momentum plume rises, ISC-PRIME stopped in the middle of execution and reported an exponentiation error. The problem was reported to EPRI. The revised source and executable code was received but not in time to revise this part of this Consequences Analysis.

Overall, the ISC-PRIME model calculates conservative results that appear to give better overall estimates than ISCST3. The design objectives of PRIME appear to have been met.

6. REFERENCES

Huber, A.H. and W.H. Snyder, 1982. Wind Tunnel Investigation of the Effects of a Rectangular Shaped Building on Dispersion of Effluents from Short Adjacent Stacks. Atm. Env.,16: 2837-2948.

Irwin, J.S., 1998. Private Communication.

Paine, Robert J., and Lew, Francis, 1997. Results of the Independent Evaluation of ISCST3 and ISC-PRIME. TR-2460026: Final Report. Prepared for Electric Power Research Institute, Palo Alto, CA.

Paine, Robert J., and Lew, Francis, 1997. Consequences Analysis for ISC-PRIME. TR-2460026: Final Report. Prepared for Electric Power Research Institute, Palo Alto, CA.

Schulman, Lloyd, 1998. Private Communication.

Schulman, L.L., D.G. Strimaitis, and J.S. Scire, 1998. Development and Evaluation of the PRIME Plume Rise and Building Downwash Model. Paper No. 4B.1, presented at the 10th Joint Conference on the Applications of air Pollution Meteorology, Phoenix, AZ.

U.S. Environmental Protection Agency, 1995a. User's Guide for the Industrial Source Complex (ISC) Dispersion Models (Revised), Volume 1, 2, and 3. EPA Publication Nos. EPA-454/B-95-003a-c. Office of Air Quality Planning and Standards, Research Triangle Park, NC.

U.S. Environmental Protection Agency, 1995b. SCREEN3 Model User's Guide. EPA Publication No. EPA-454/B-95-004. Office of Air Quality Planning and Standards, Research Triangle Park, NC.

Weil, J.C., 1996. A New Dispersion Model for Stack Sources in Building Wakes, Ninth Joint Conference on Application of Air Pollution Meteorology with A&WMA, 333-337, American Meteorological Society, Boston, MA.

APPENDIX A

CONSEQUENCES ANALYSIS SOURCE PARAMETERS

The following two sets of point source emissions data were also the data used in the EPRI Consequences Analysis:

Parameter		Stack 1	Stack2
Stack Height (m)	:	35.0	100.0
Emission Rate (g/s)	:	100.0	100.0
Exit Temperature (K)	:	432.0	416.0
Exit Velocity (m/s)	:	11.7	18.8
Stack Diameter (m)	:	2.4	4.6

The last set of point source emission data were the values that had caused ISC-PRIME to crash. When raising the exit velocity to 10.1, the program ran just fine. The problem was identified corrected by the developers.

Parameter		Stack 3
Stack Height (m)	:	5.0
Emission Rate (g/s)	:	10.0
Exit Temperature (K)	:	280.0
Exit Velocity (m/s)	:	1.1
Stack Diameter (m)	:	2.4

APPENDIX B

TABLE OF CONSEQUENCES ANALYSIS SCENARIOS.

ISC-PRIME Consequence Analysis: Modeling Scenarios

Case	Bldg. Dimensions	Bldg. Ht. (m)	Dispersion	Stack Ht. (m)
No Building	N/A	N/A	Urban	35
			Rural	35
		N/A	Urban	100
			Rural	100
Squat Building Stack Adjacent to NE Corner of Building	60m x 120m	34	Urban	35
			Rural	35
		50	Urban	100
			Rural	100
Squat Building Stack at 4xHb to NE Corner of Building	60m x 120m	34	Urban	35
			Rural	35
		50	Urban	100
			Rural	100
Tall Building Stack Adjacent to NE Corner of Building	30m x 30m	34	Urban	35
			Rural	35
		50	Urban	100
			Rural	100
Tall Building Stack at 4xHb to NE Corner of Building	30m x 30m	34	Urban	35
			Rural	35
		50	Urban	100
			Rural	100
Super Squat Building Stack Adjacent to NE Corner of Building	180m x 180m	34	Urban	35
			Rural	35
Super Squat Building Stack at 4xHb to NE Corner of Building	180m x 180m	34	Urban	35
			Rural	35

APPENDIX C

VARIOUS FIGURES

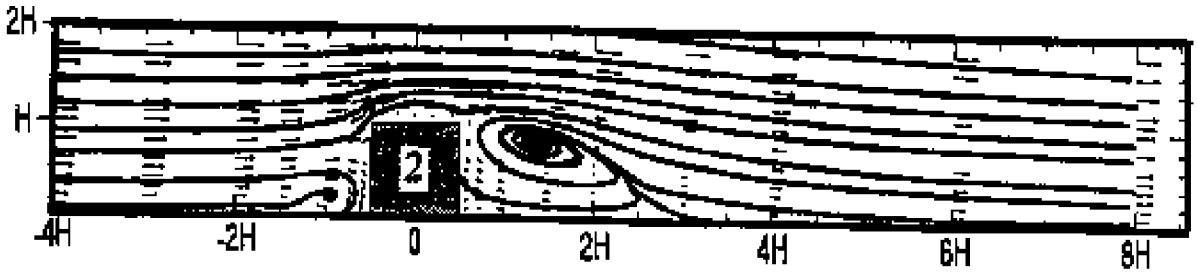

Figure 1. Streamlines around a building (2). Wind flow is from left to right.

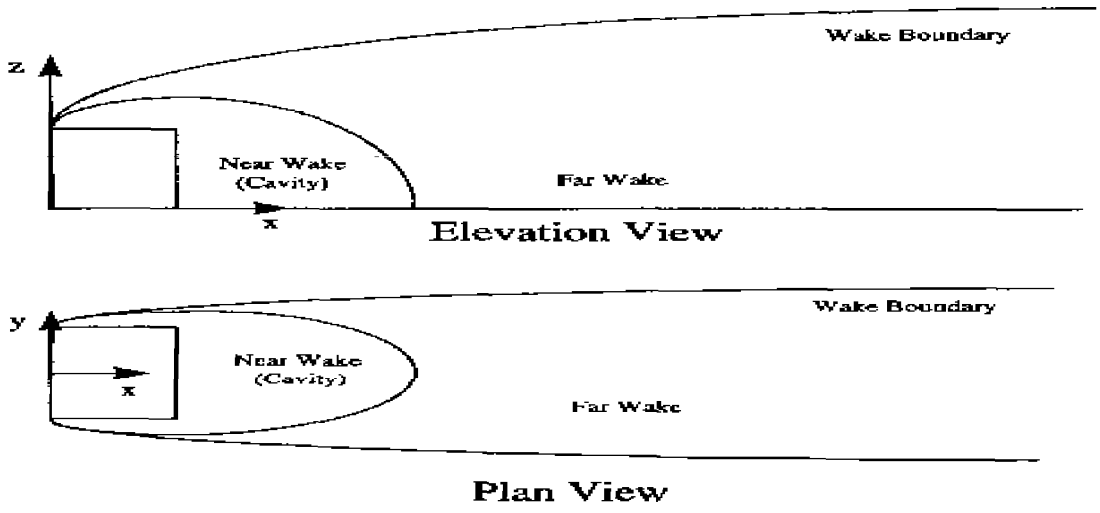

Figure 2. Depiction of ellipsoidal shape of Near Wake (cavity), Far Wake, and Wake Boundary.

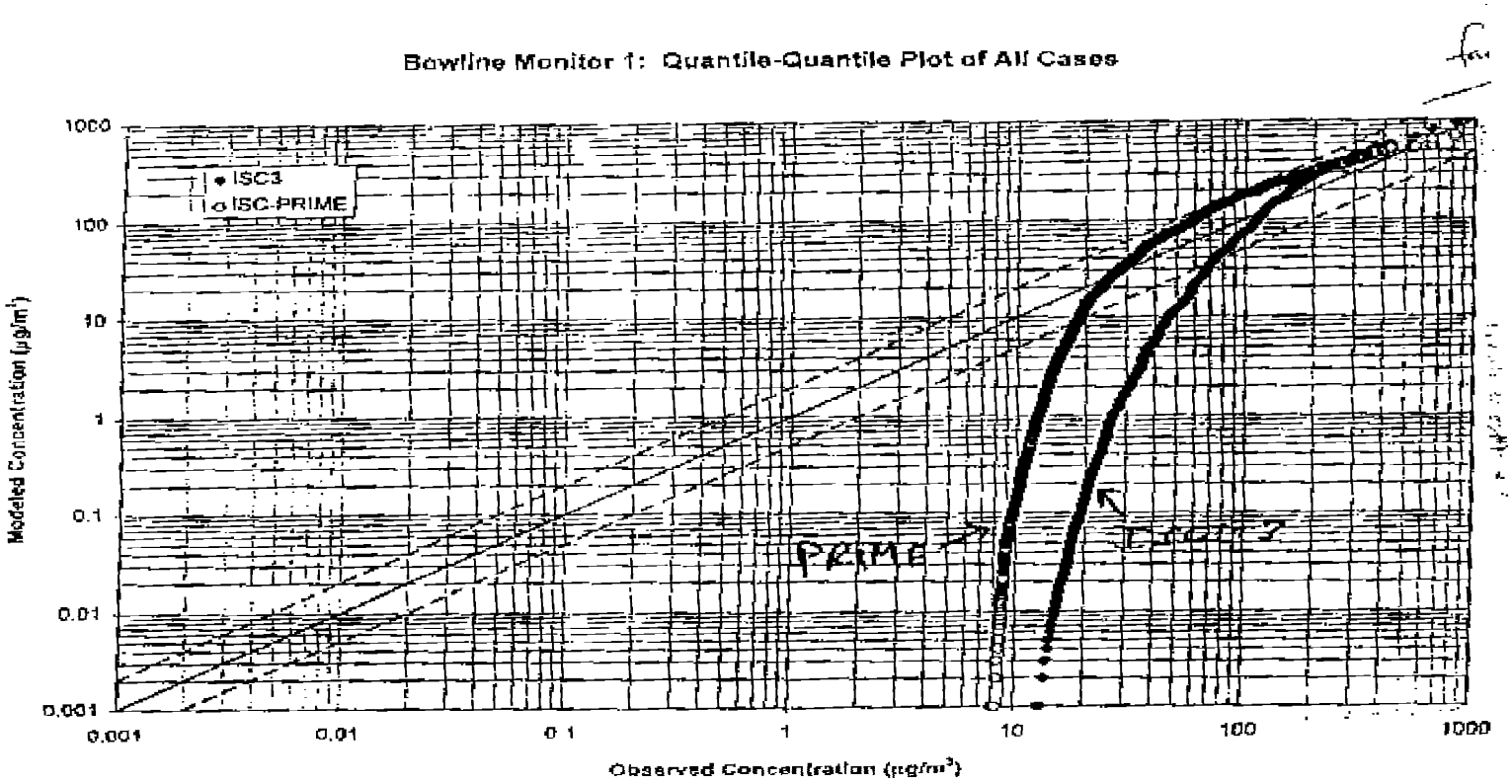

Figure 3. Bowline Monitor 1: Quantile-Quantile Plot of All Cases. Note dashed factor of 2 lines, one on either side of the 1:1 ratio line cutting diagonally across from corner to corner.

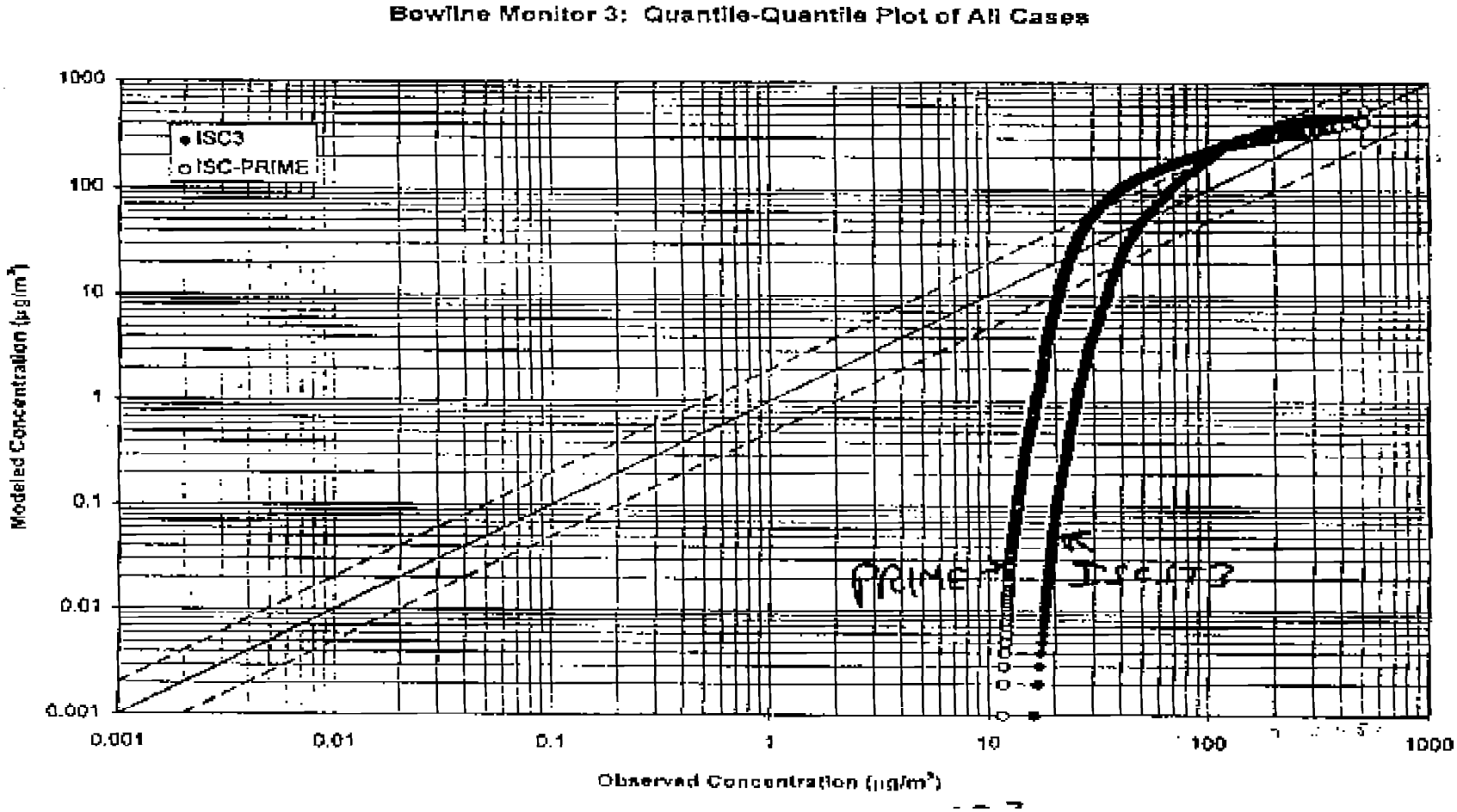

Figure 4. Bowline Monitor 3: Quantile-Quantile Plot of All Cases. Note dashed factor of 2 lines, one on either side of the 1:1 ratio line cutting diagonally across from corner to corner. Note also that the PRIME curve goes above the 1:1 line by about a factor of 3.

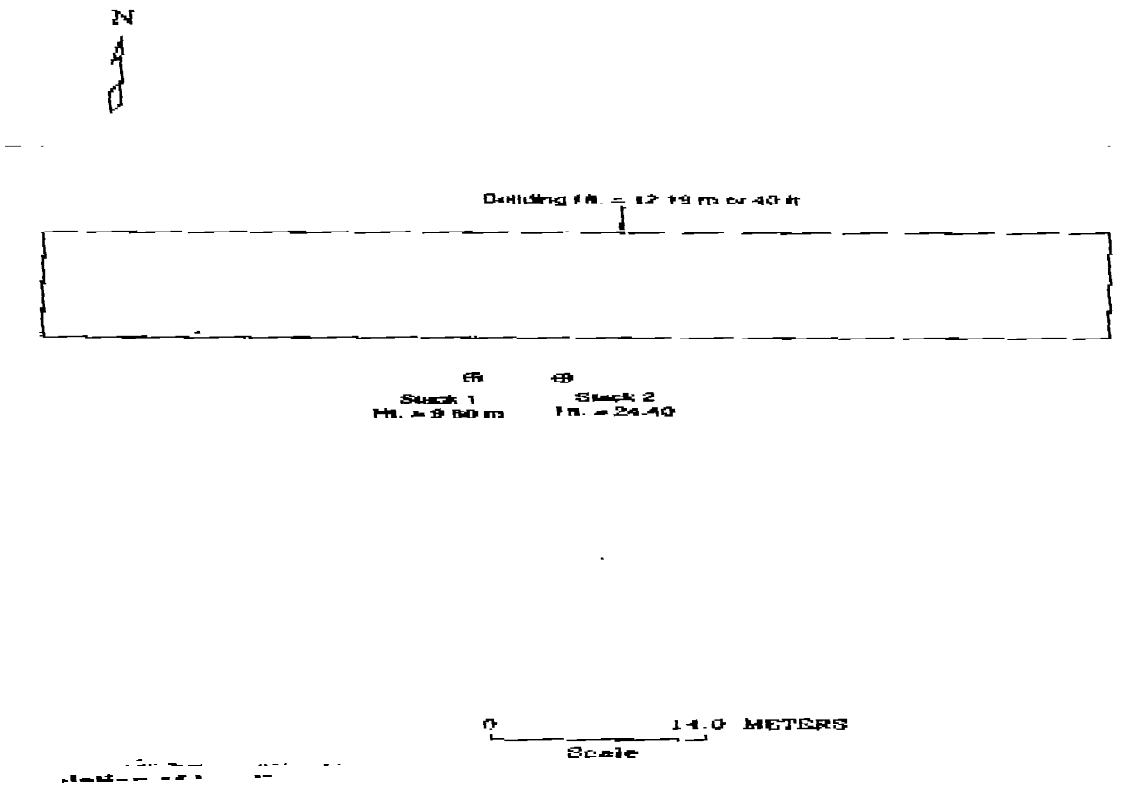

Figure 5a. Depiction of locations of the building and stacks used for the BPIP processing for the AGA data base: Kansas site. The building is 12.19 m high and the stack heights are 9.8 m and 24.4m high.

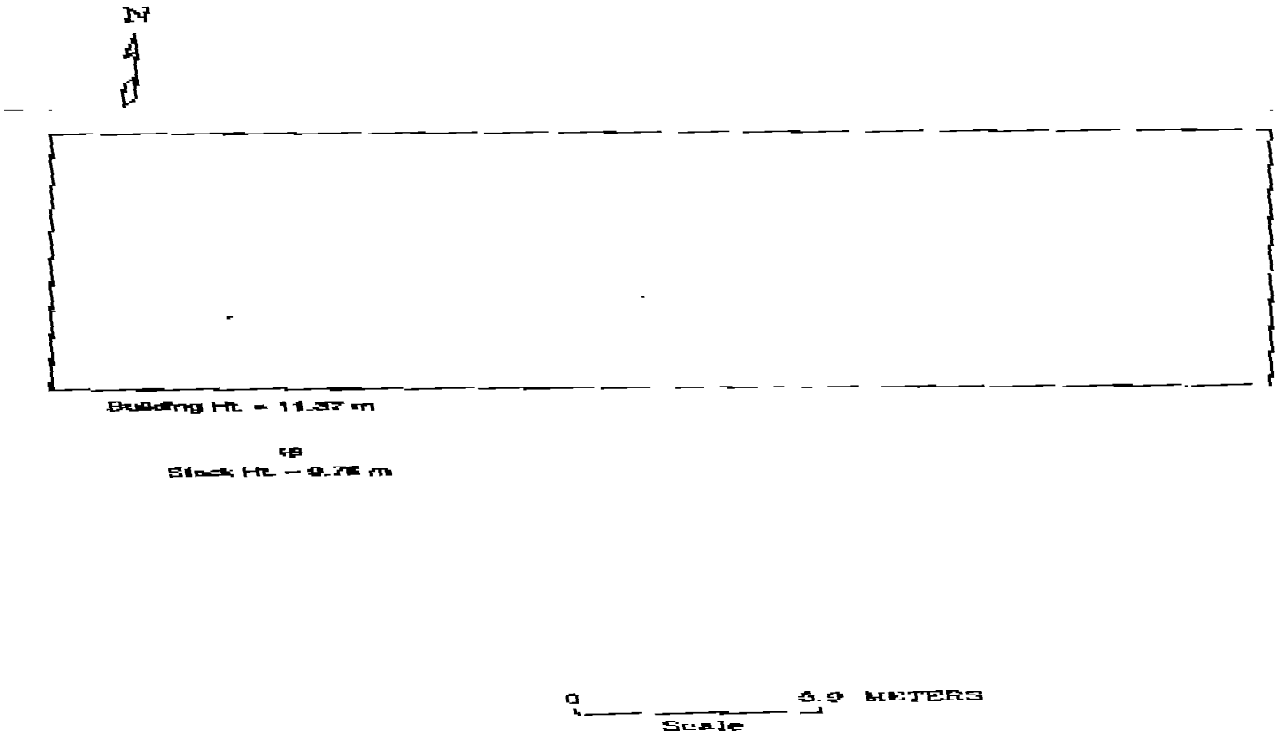

Figure 5b. Depiction of locations of the building and stacks used for the BPIP processing for the AGA data base: Texas site. The building is 11.37 m high and the stack is 9.75 m high.

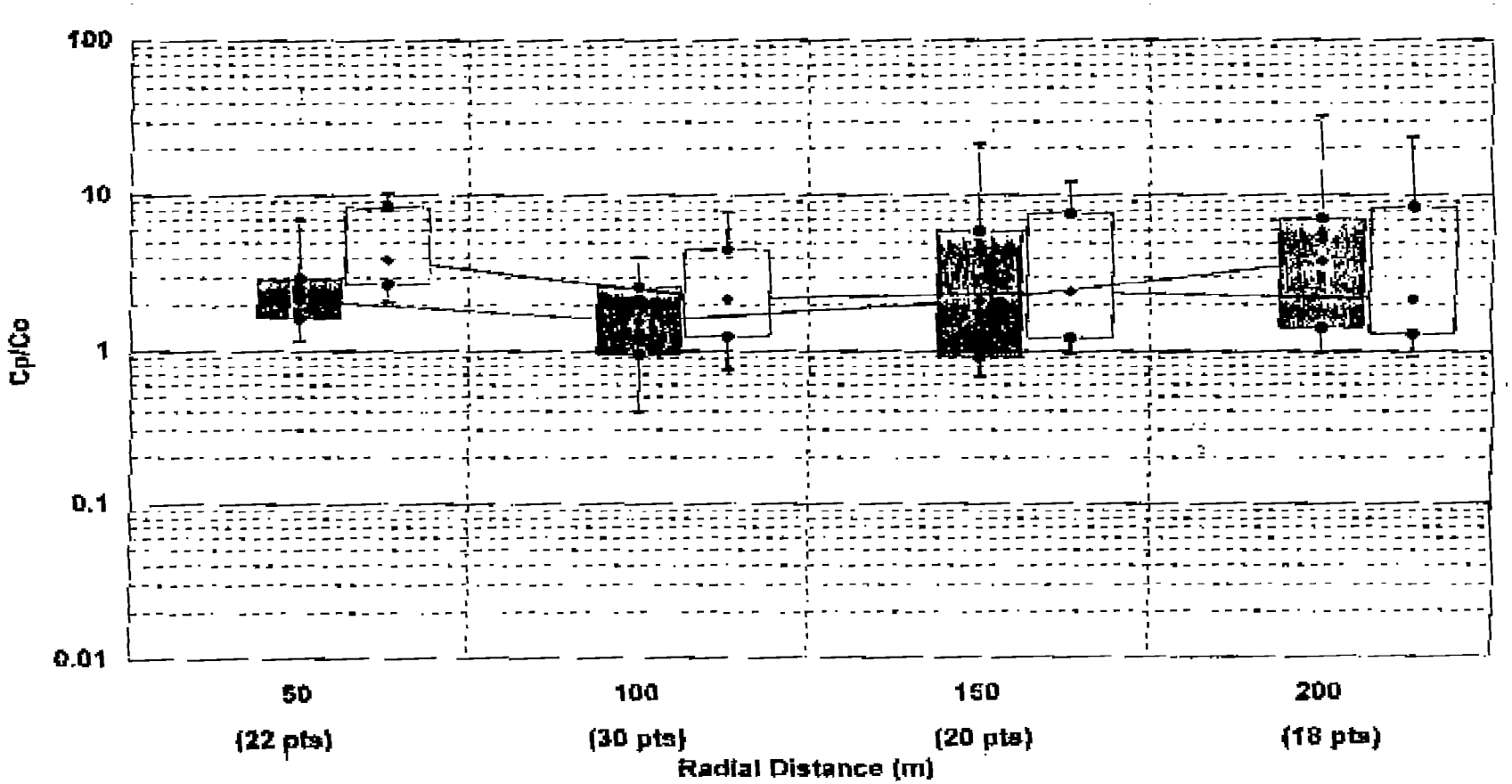

Figure 6. Residual plot of predicted to observed concentration ratios versus distance for the AGA data base. The filled in rectangles represent ISC-PRIME data while the transparent rectangles represent ISCST3 data.

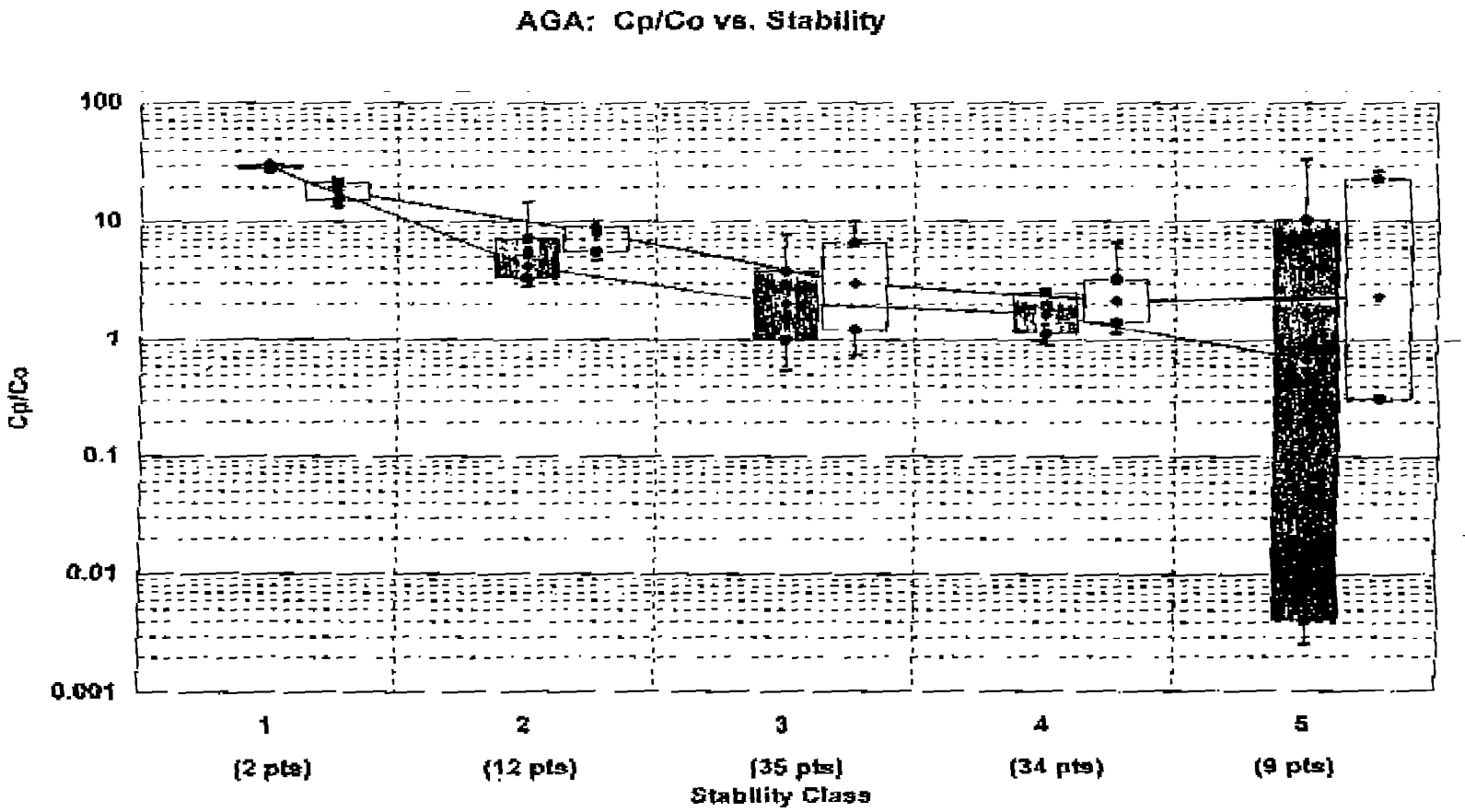

Figure 7. Residual plot of predicted to observed concentration ratios versus stability class for the AGA data base. The filled in rectangles represent ISC-PRIME data while the transparent rectangles represent ISCST3 data.

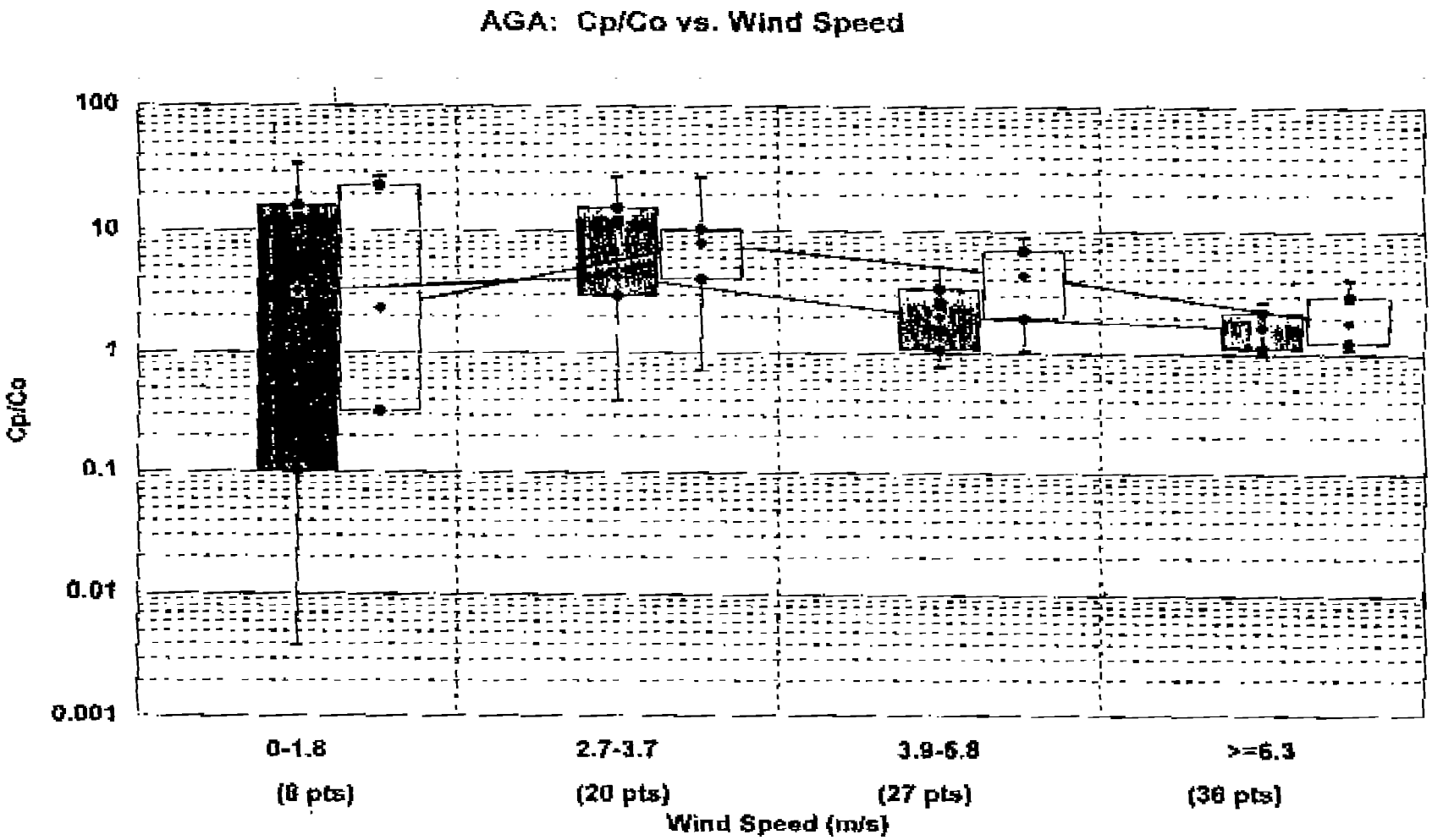

Figure 8. Residual plot of predicted to observed concentration ratios versus 10-m wind speed for the AGA data base. The filled in rectangles represent ISC-PRIME data while the transparent rectangles represent ISCST3 data.

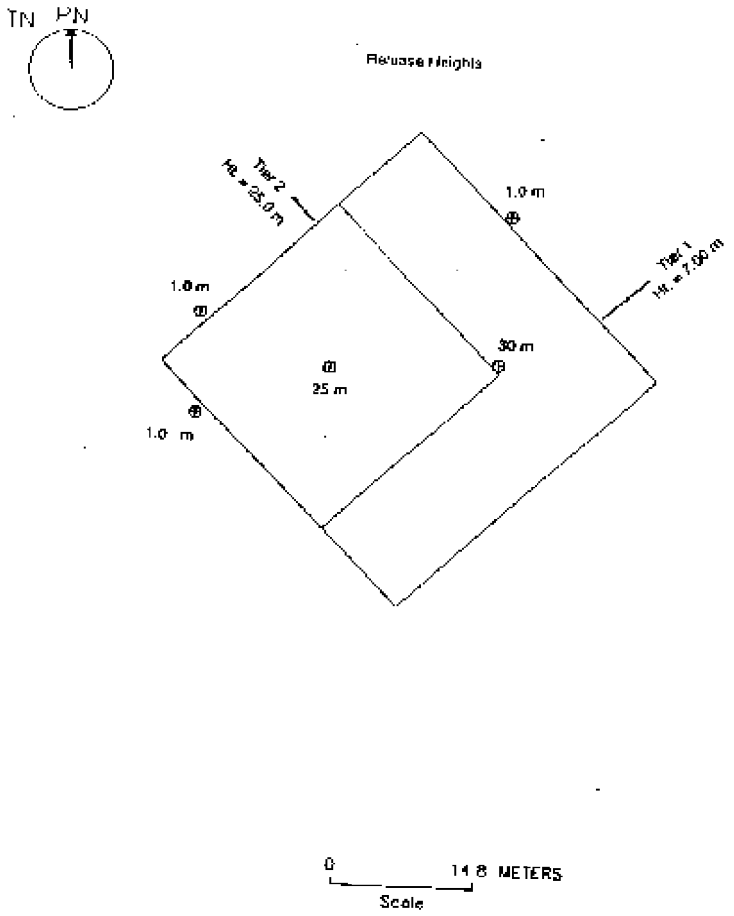

Figure 9. Depiction of locations of the building tiers and stacks used for the EOCR data base. Tier heights are 7.0 and 25 m high while stacks along the perimeter are 1 m high and stacks on the tiers are 25 m and 30 m high.

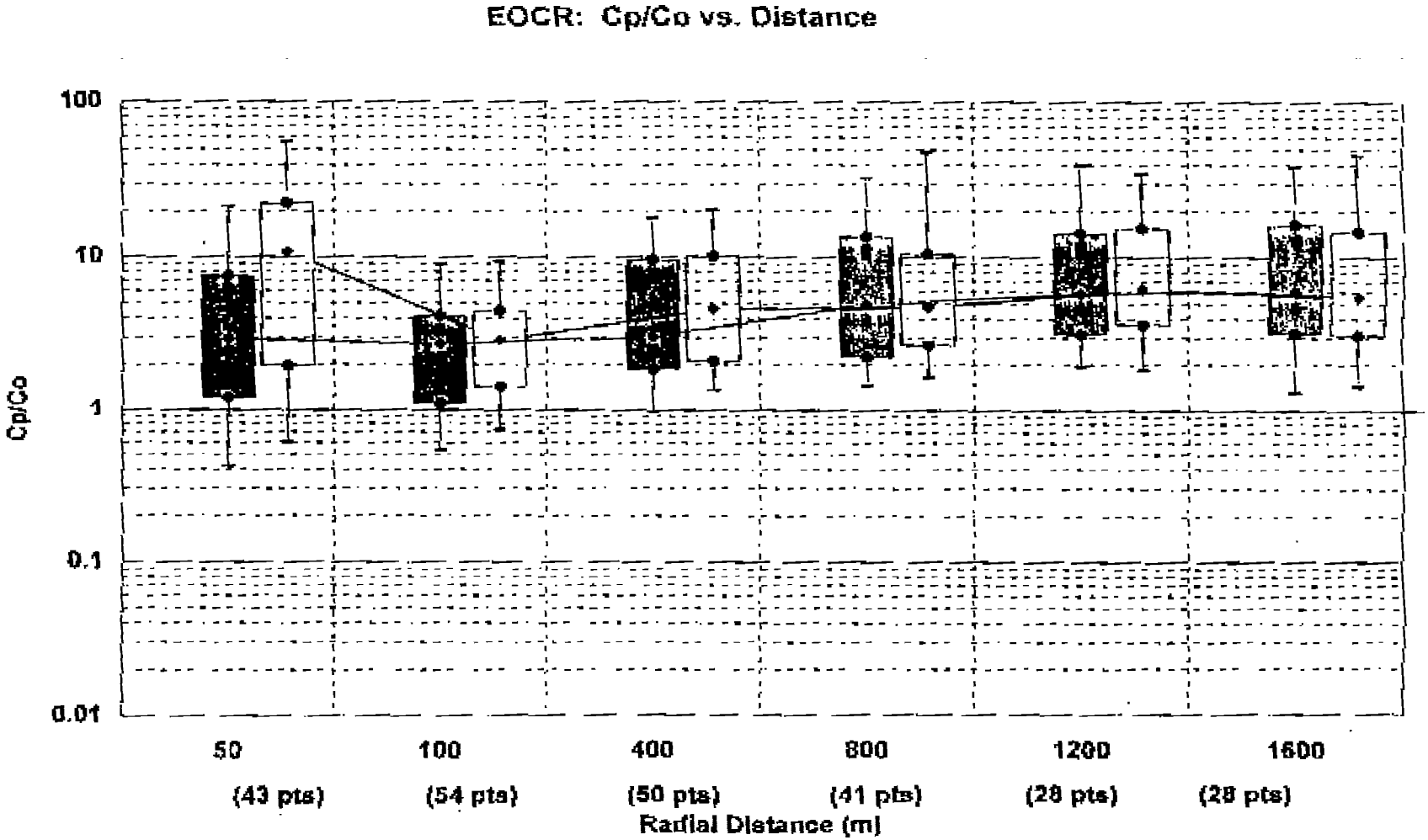

Figure 10. Residual pot of predicted to observed concentration ratios versus distance for the EOCR data base. The filled in rectangles represent ISC-PRIME data while the transparent rectangles represent ISCST3 data.

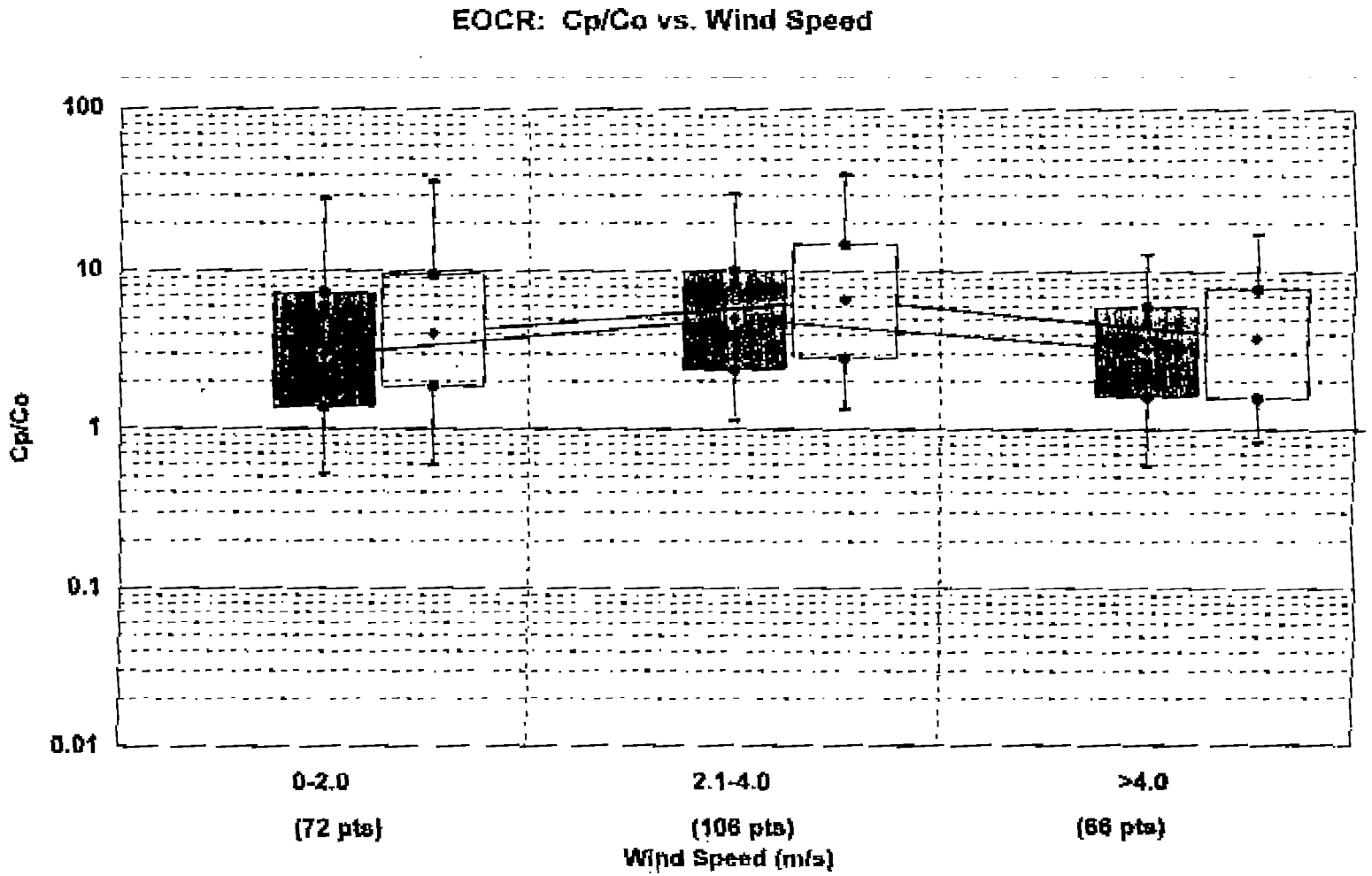

Figure 11. Residual plot of predicted to observed concentration ratios versus 10-m wind speed for the EOCR data base. The filled in rectangles represent ISC-PRIME data while the transparent rectangles represent ISCST3 data.

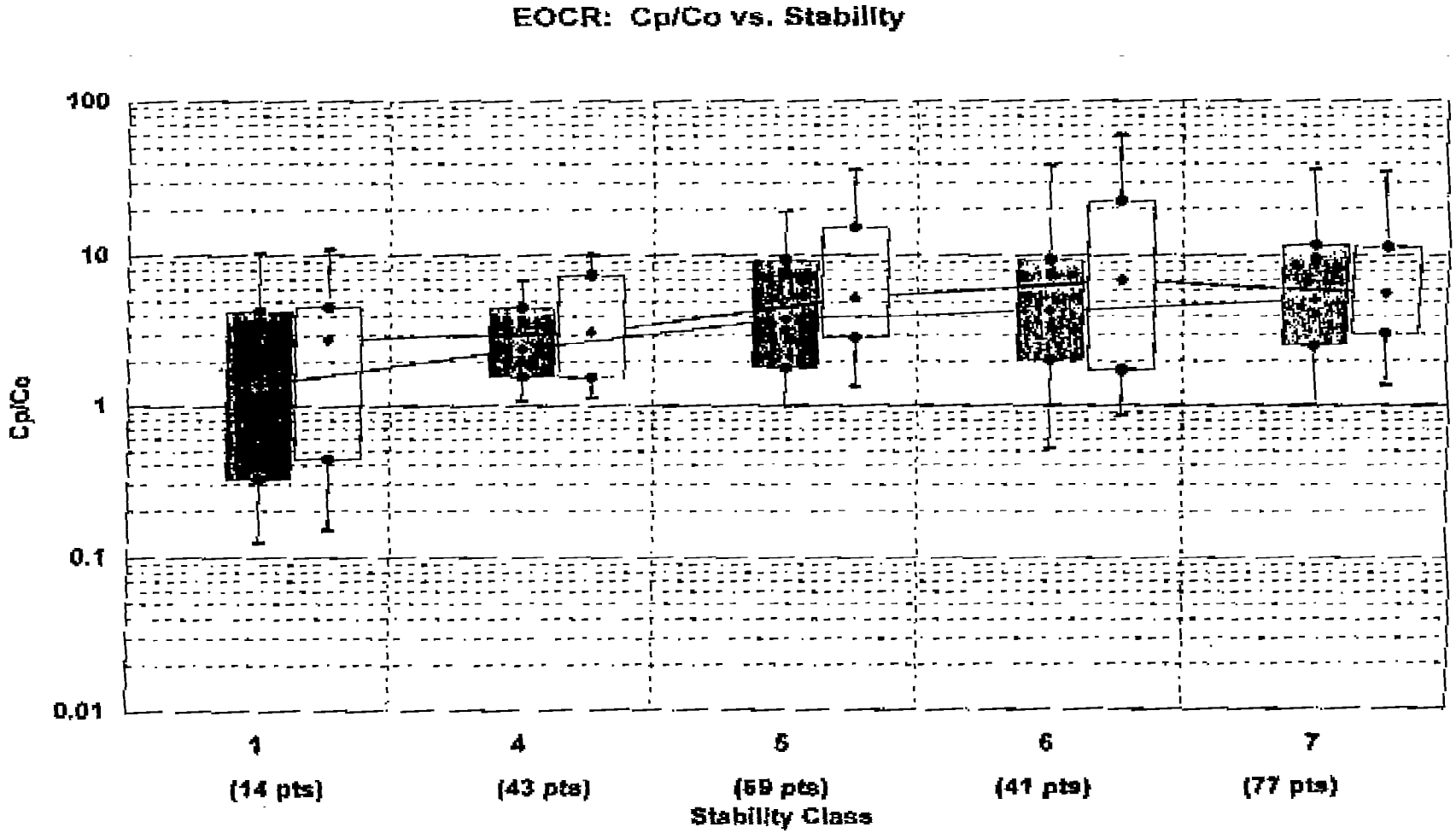

Figure 12. Residual plot of predicted over observed versus stability class for the EOCR data base. The filled in rectangles represent ISC-PRIME data while the transparent rectangles represent ISCST3 data.

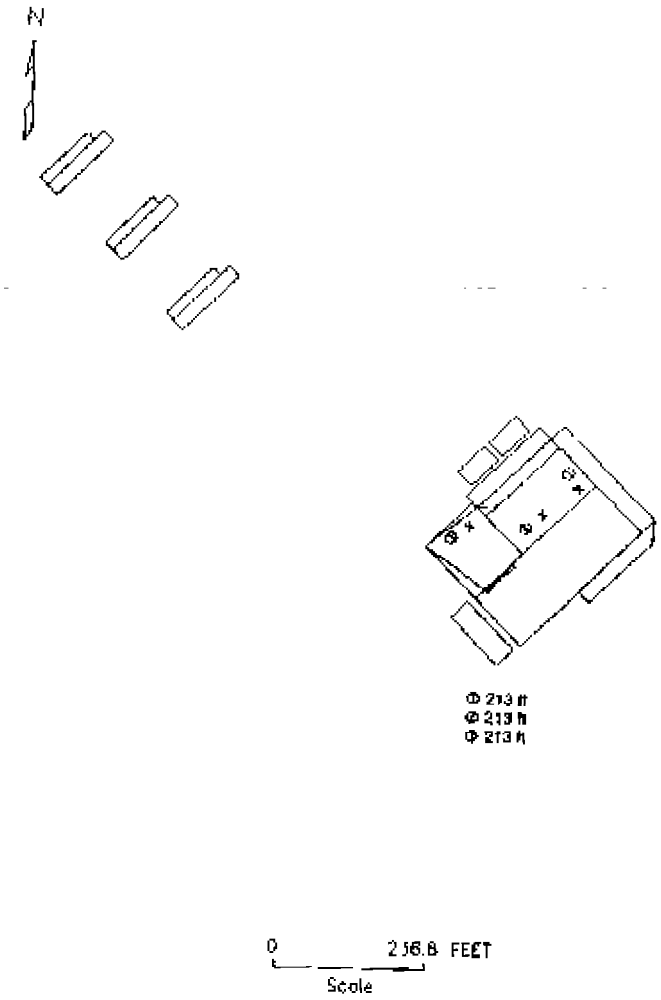

Figure 13. Depiction of all building tiers and stacks used for the BPIP processing for the Lee Power Plant data base. The stacks are 213 m high.

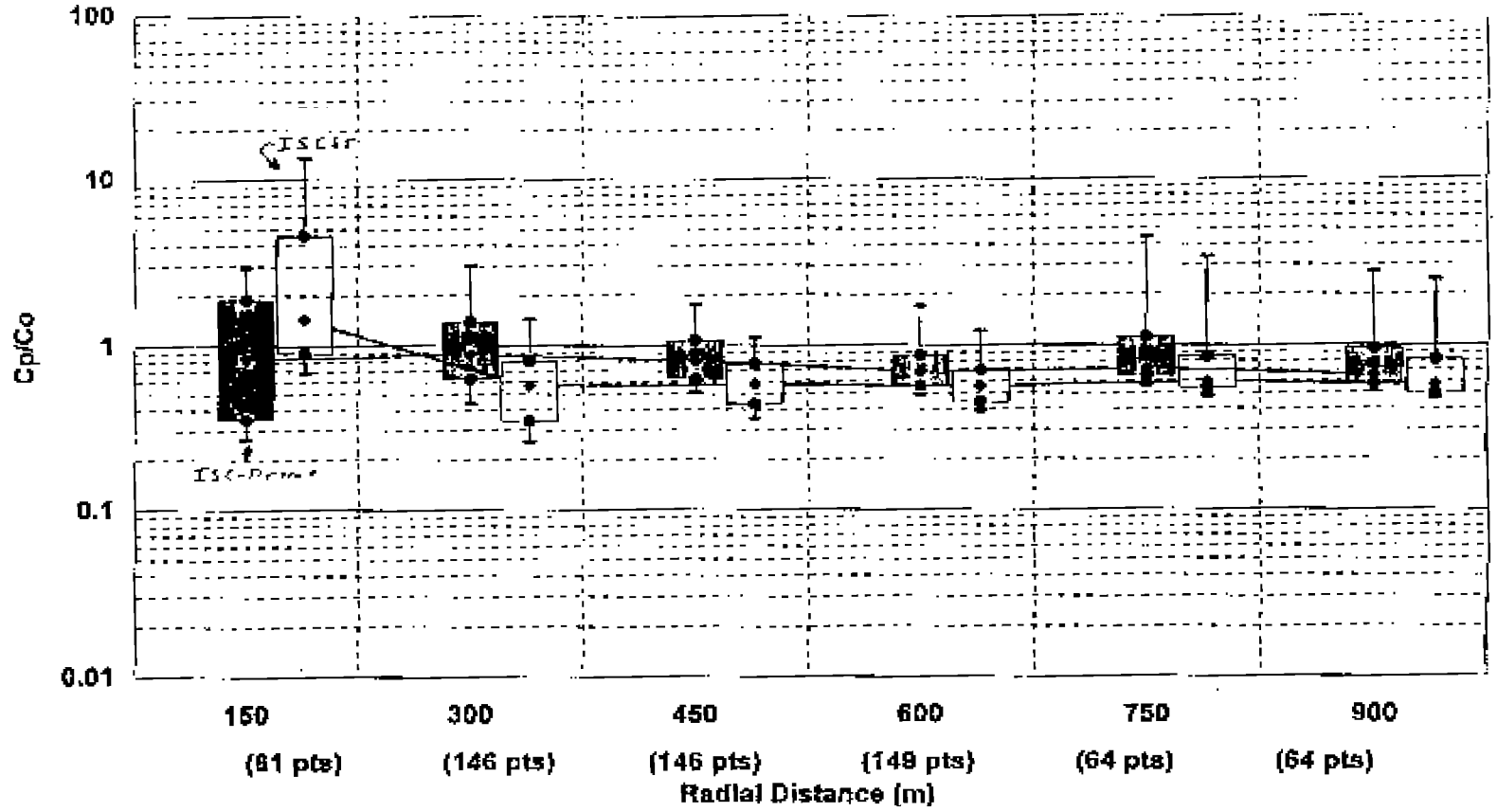

Figure 14. Residual plot of predicted over observed concentration ratios versus distance for the Lee Power Plant data base, neutral (urban) cases only. The filled in rectangles represent ISC-PRIME data while the transparent rectangles represent ISCST3 data.

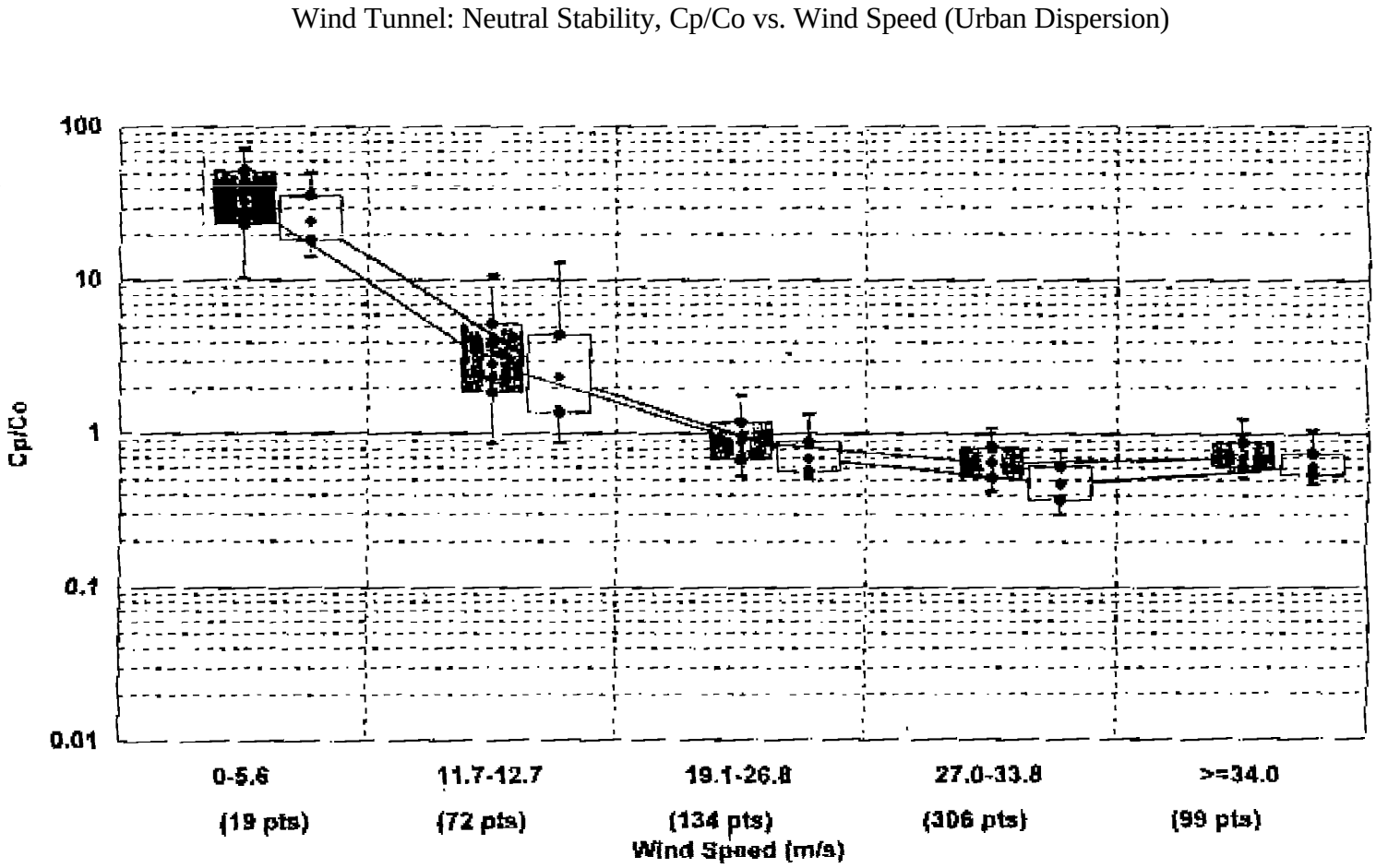

Figure 15. Residual plot of predicted over observed concentration ratios versus 10-meter wind speed for the Lee Power Plant data base, neutral (urban) cases only. The filled in rectangles represent ISC-PRIME data while the transparent rectangles represent ISCST3 data.

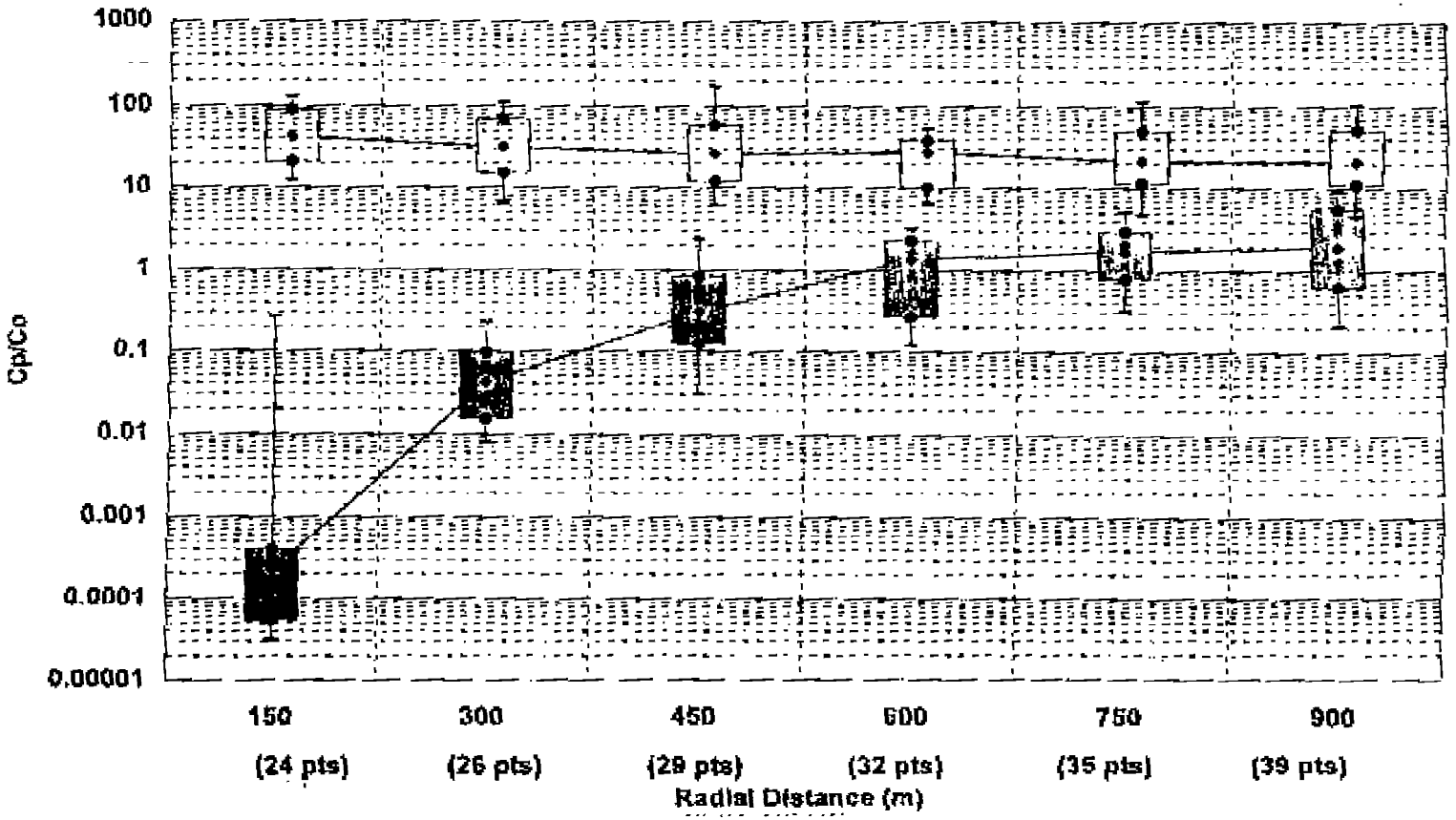

Figure 16. Residual plot of predicted over observed concentration ratios versus distance for the Lee Power Plant data base, stable (rural) cases only. The filled in rectangles represent ISC-PRIME data while the transparent rectangles represent ISCST3 data.

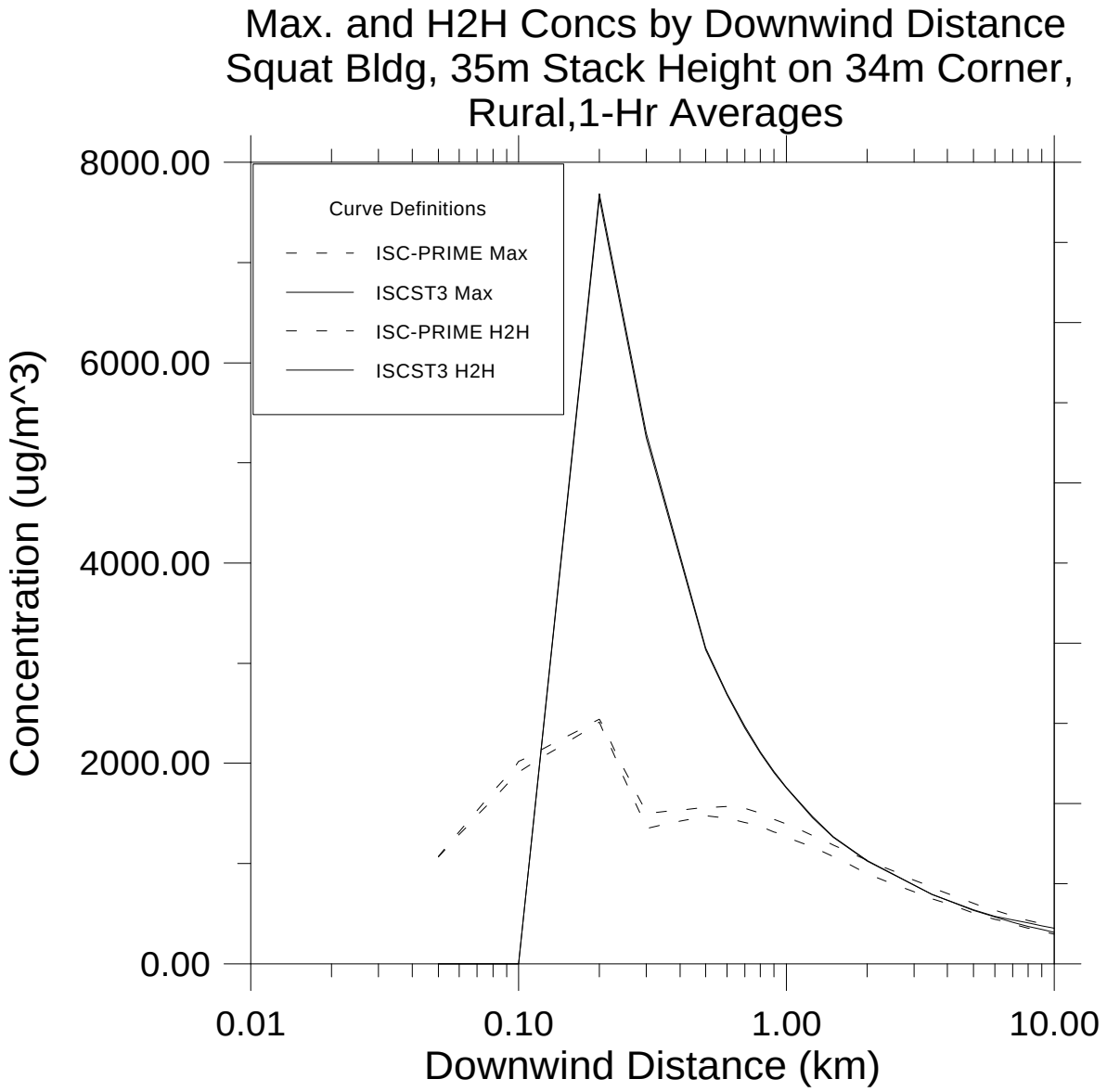

Figure 17. Maximum and Highest of the Second Highest 1-hour averaged concentrations versus downwind distance. ISCST3 max and H2H coincide visually.

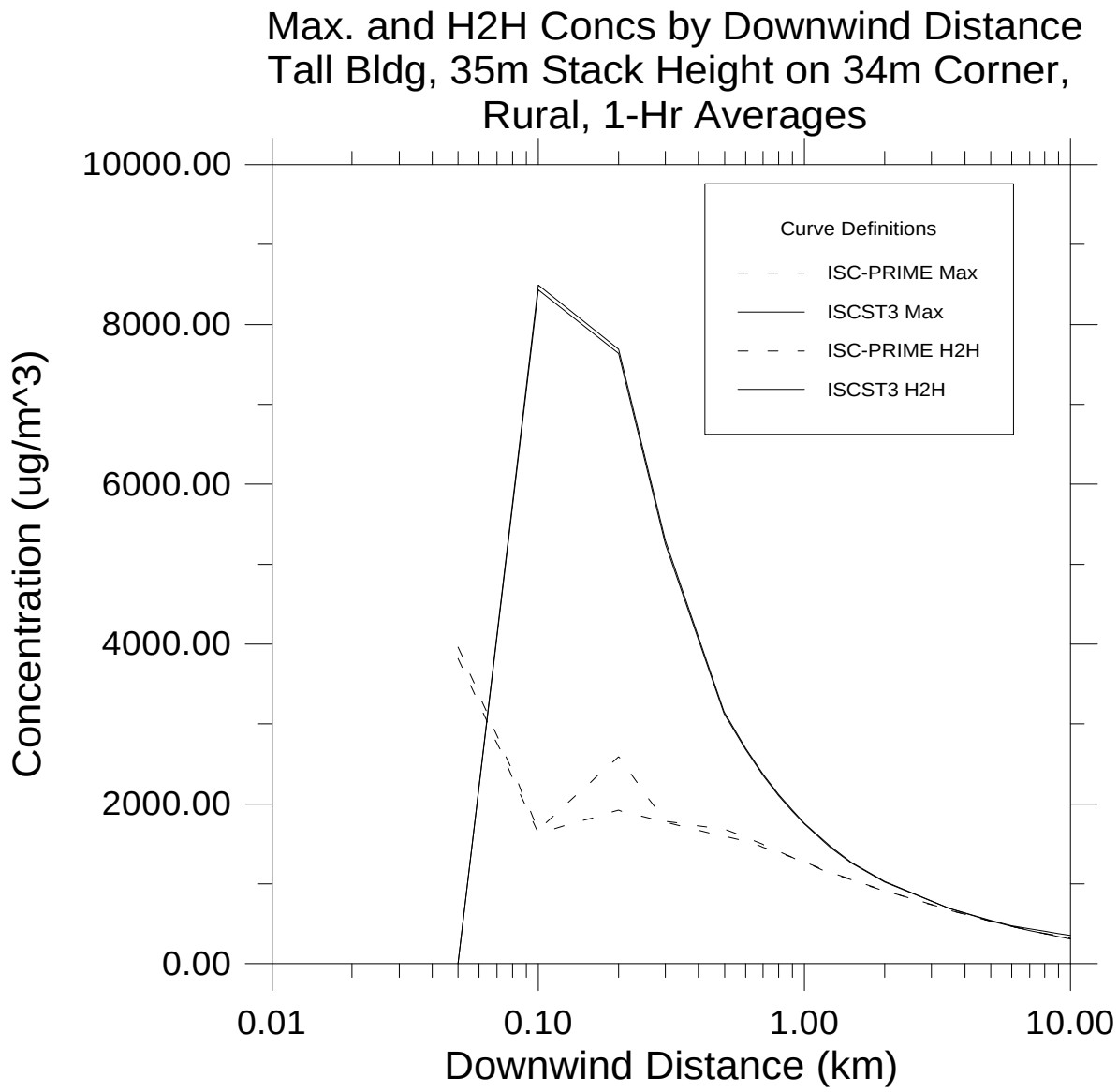

Figure 18. Maximum and Highest of the Second Highest 1-hour averaged concentrations versus downwind distance. ISCST3 max and H2H coincide visually over much of the ISCST3 curves.

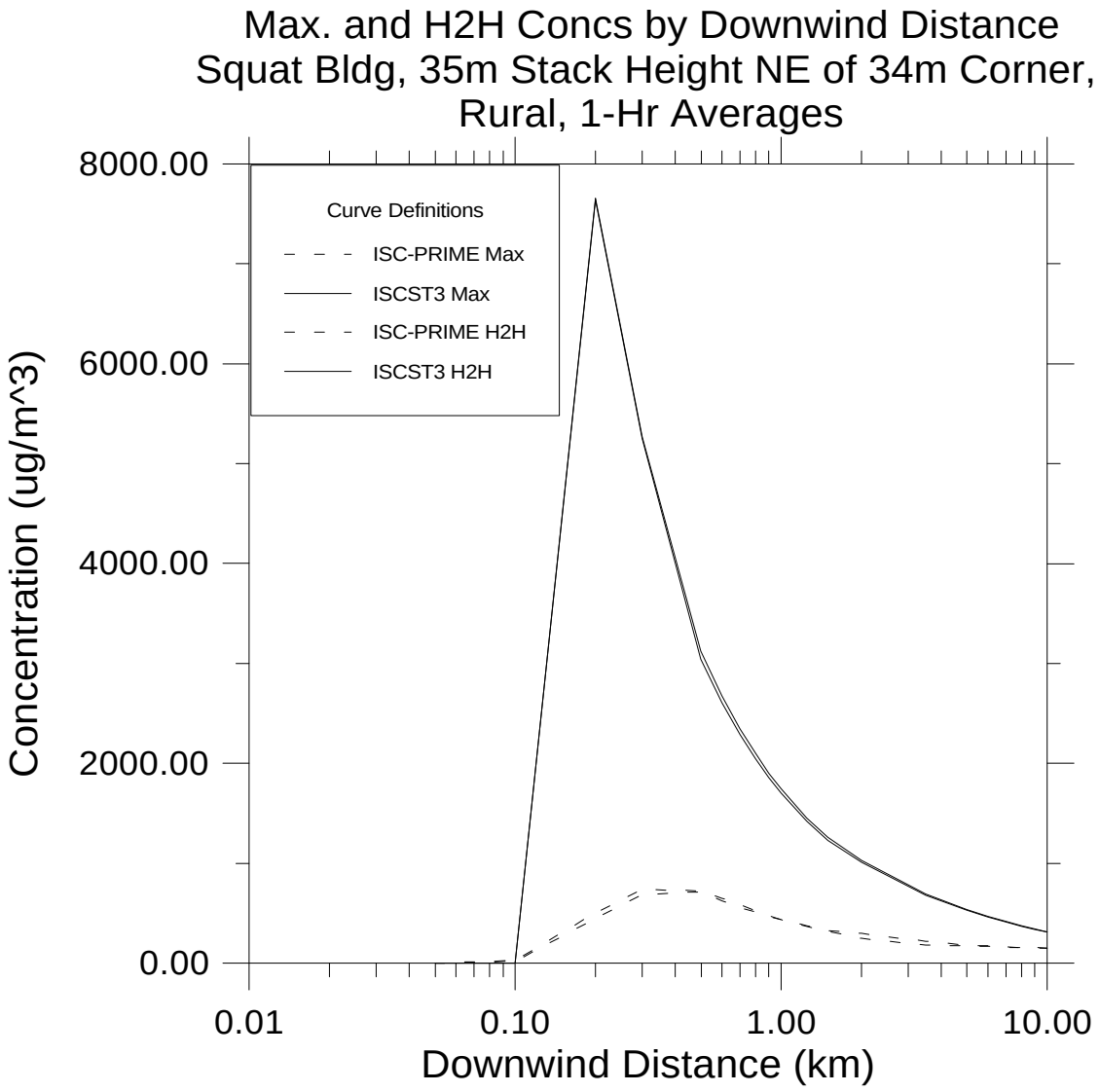

Figure 19. Maximum and Highest of the Second Highest 1-hour averaged concentrations versus downwind distance. ISCST3 max and H2H coincide visually over much of the ISCST3 curves.

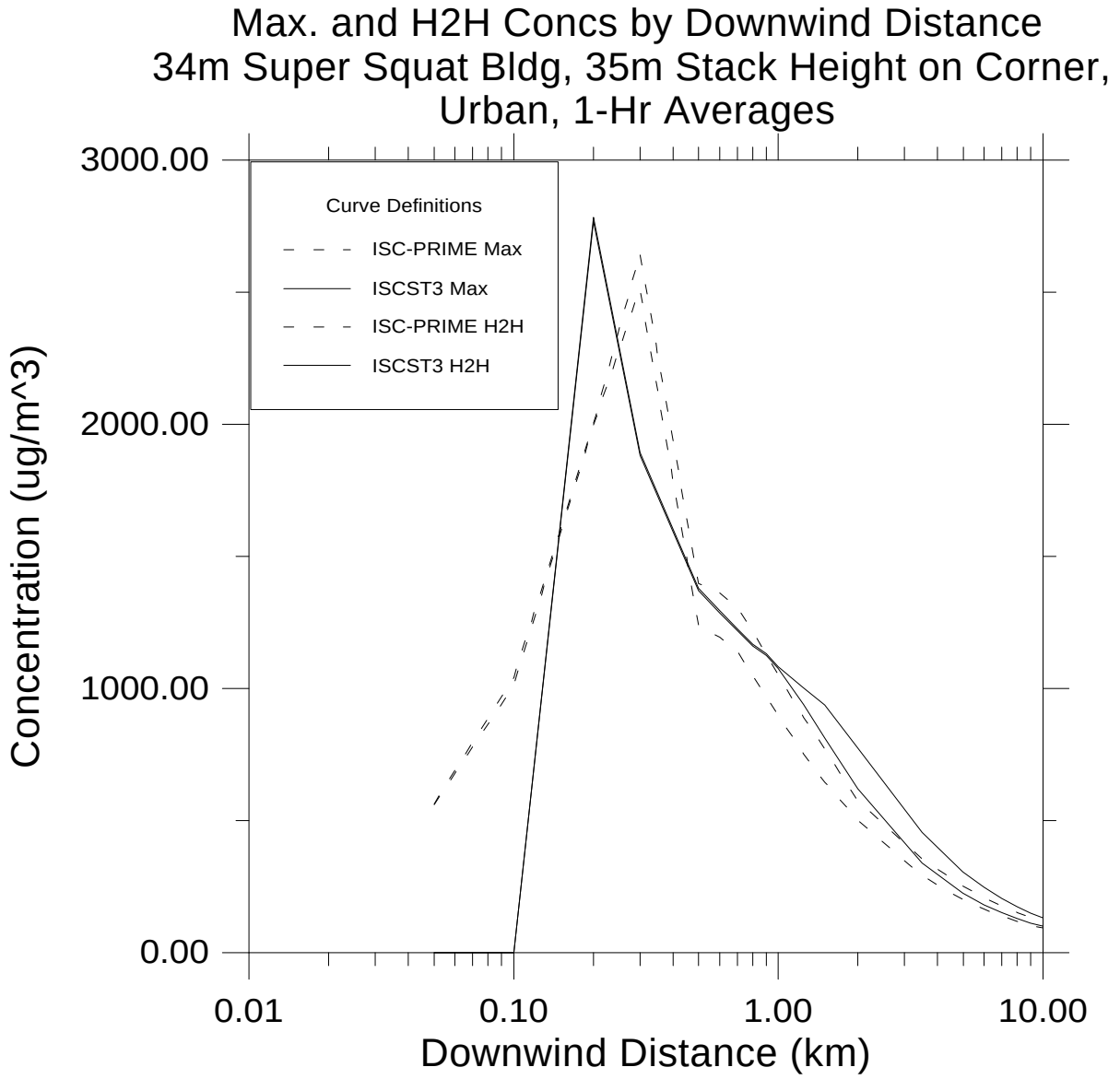

Figure 20. Maximum and Highest of the Second Highest 1-hour averaged concentrations versus downwind distance.

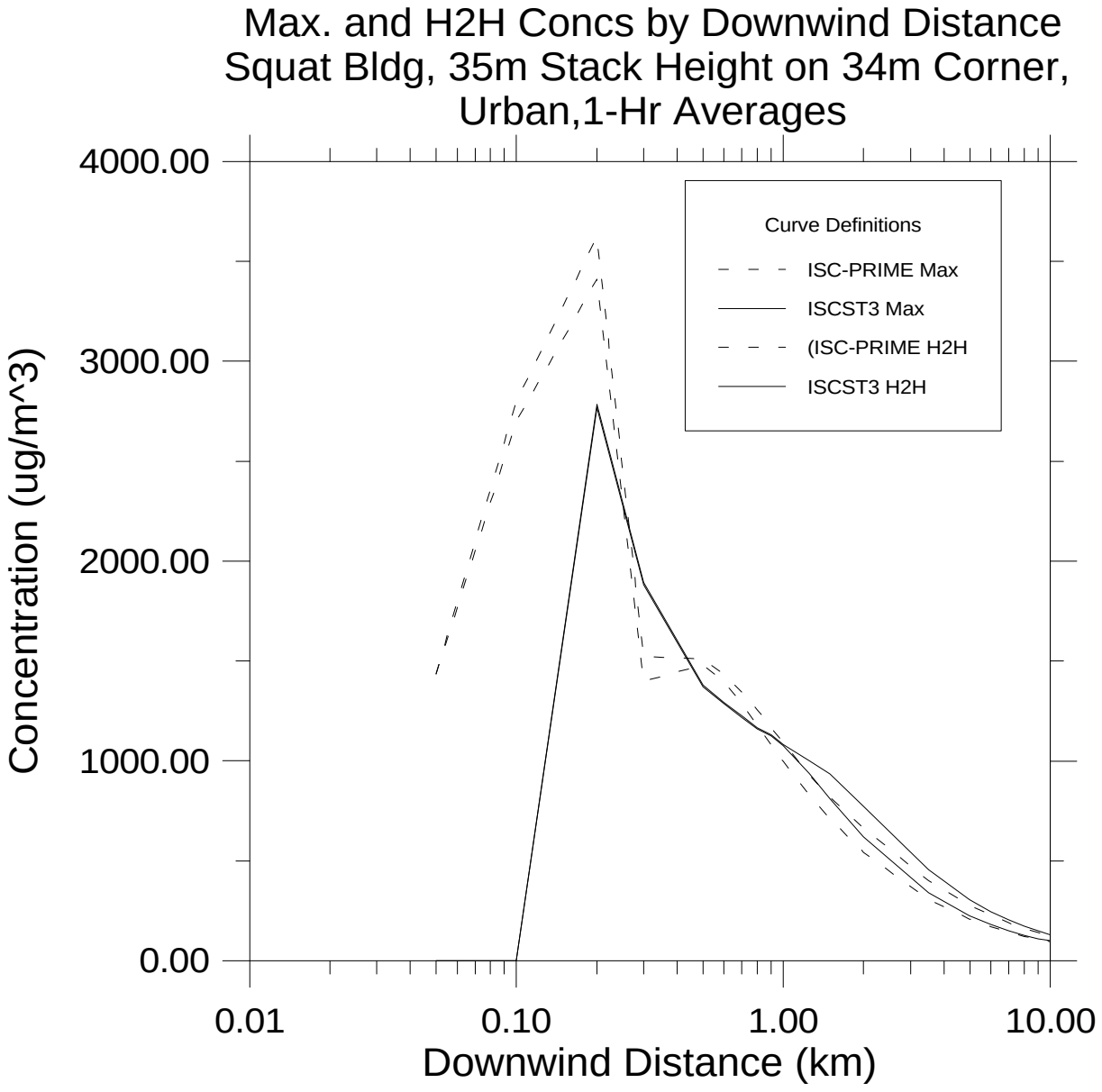

Figure 21. Maximum and Highest of the Second Highest 1-hour averaged concentrations versus downwind distance.

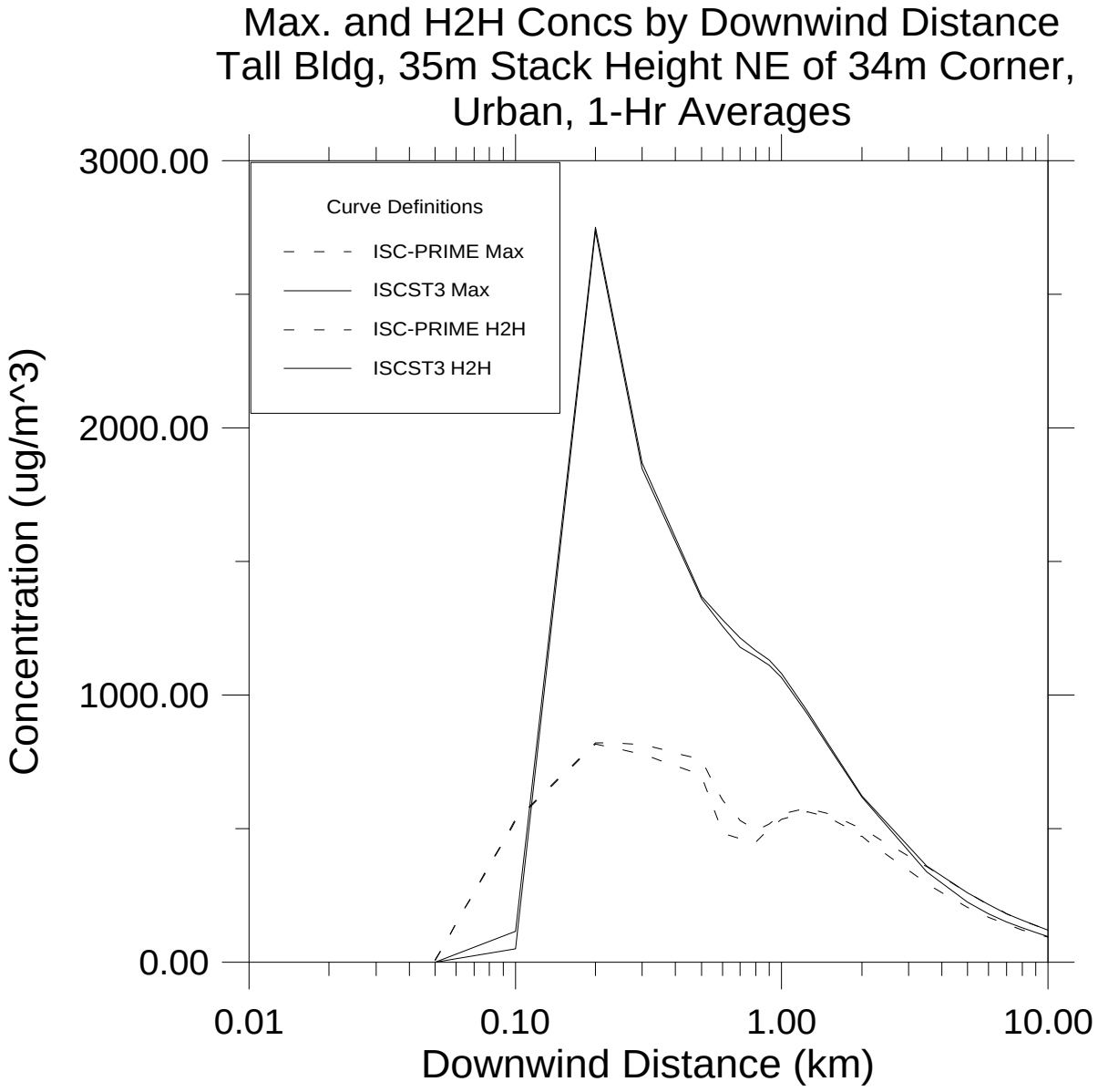

Figure 22. Maximum and Highest of the Second Highest 1-hour averaged concentrations versus downwind distance.

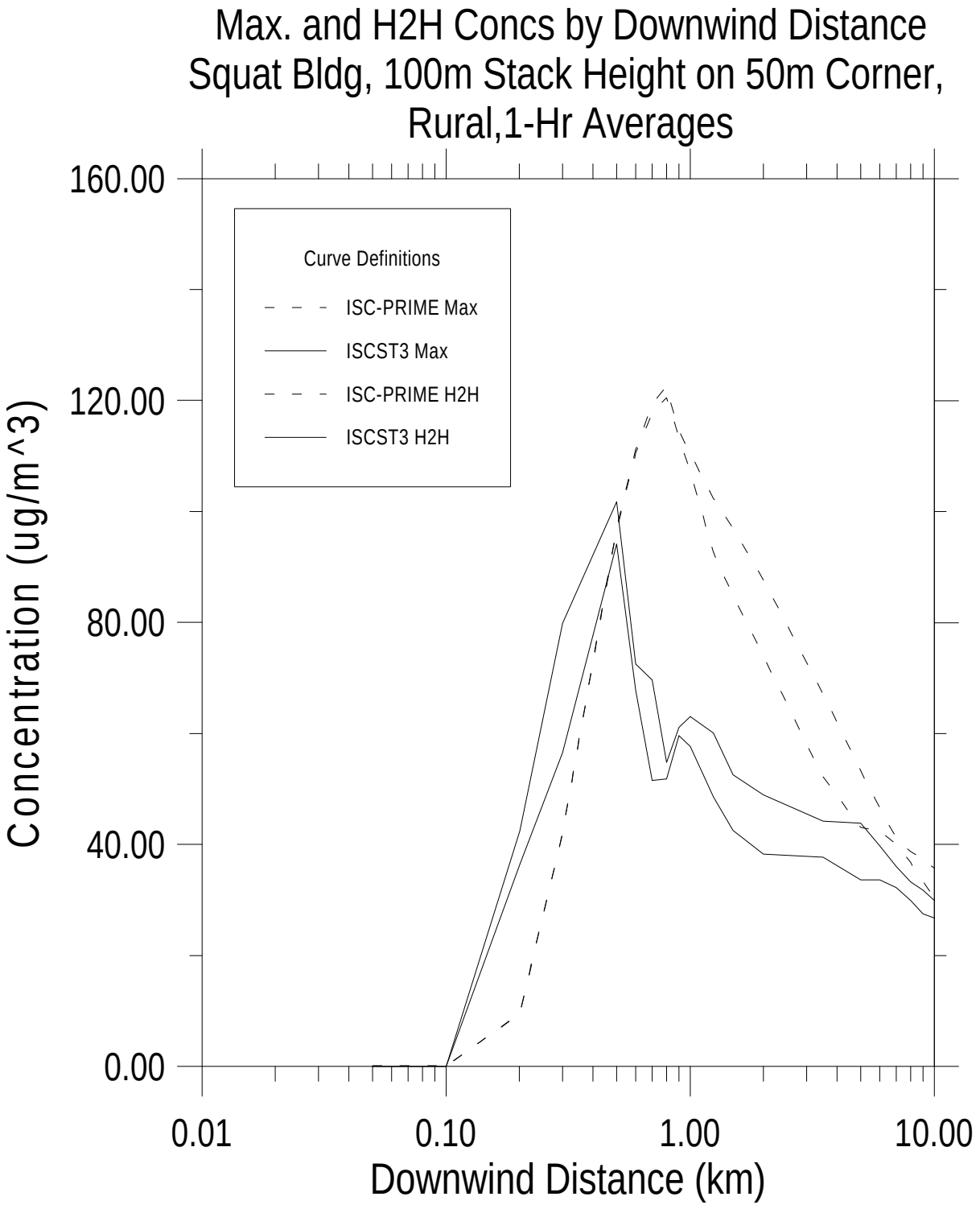

Figure 23. Maximum and Highest of the Second Highest 1-hour averaged concentrations versus downwind distance.

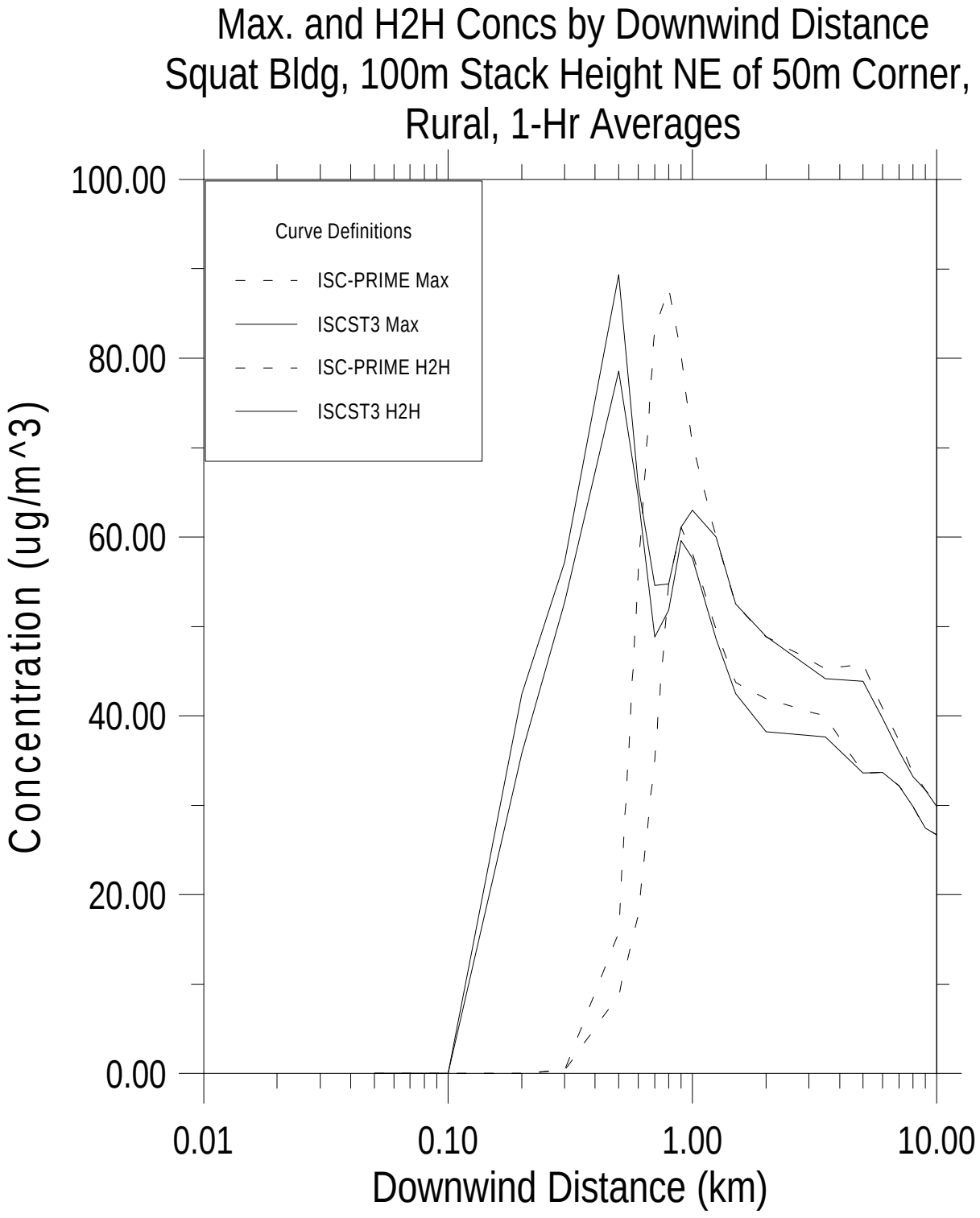

Figure 24. Maximum and Highest of the Second Highest 1-hour averaged concentrations versus downwind distance.

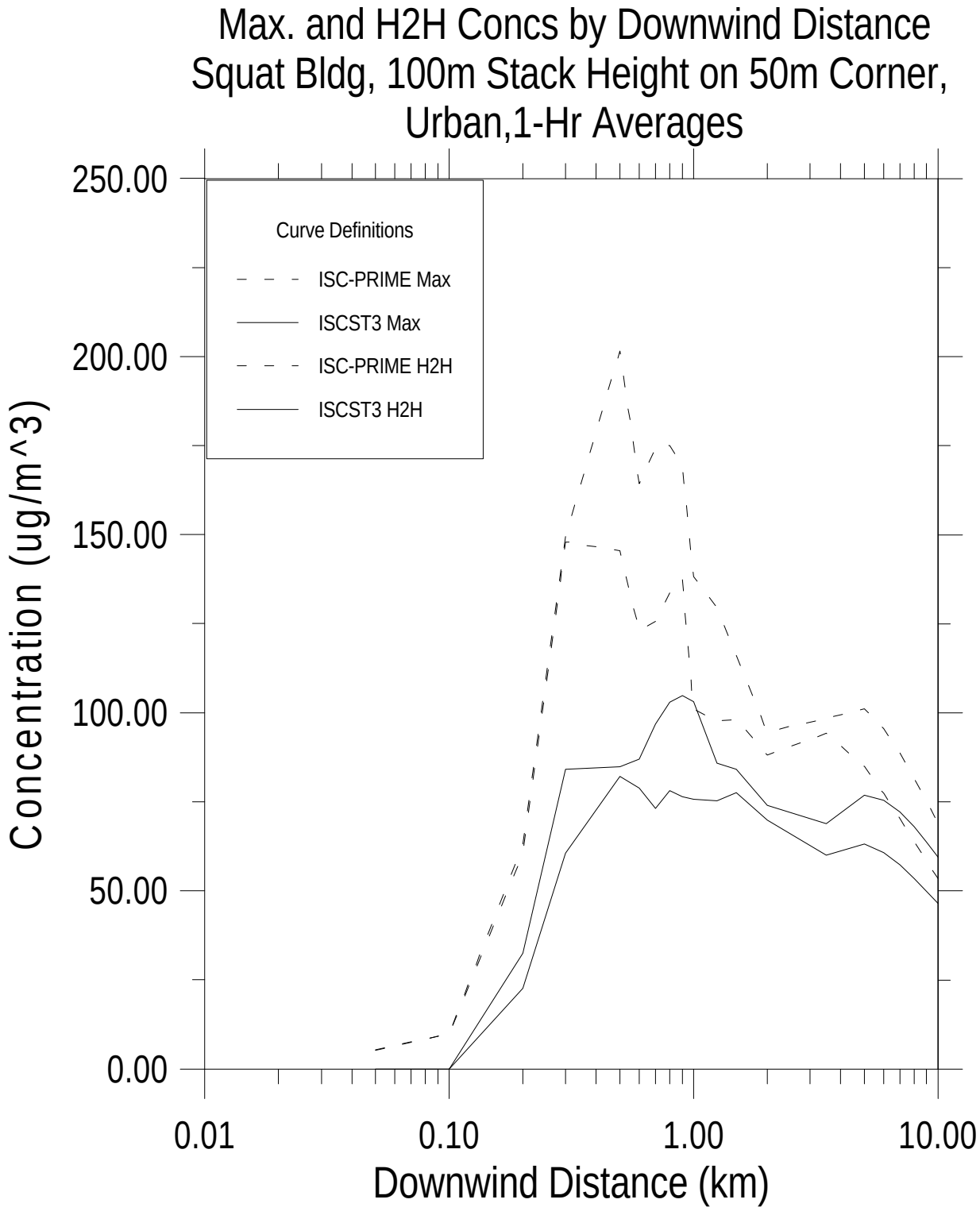

Figure 25. Maximum and Highest of the Second Highest 1-hour averaged concentrations versus downwind distance.

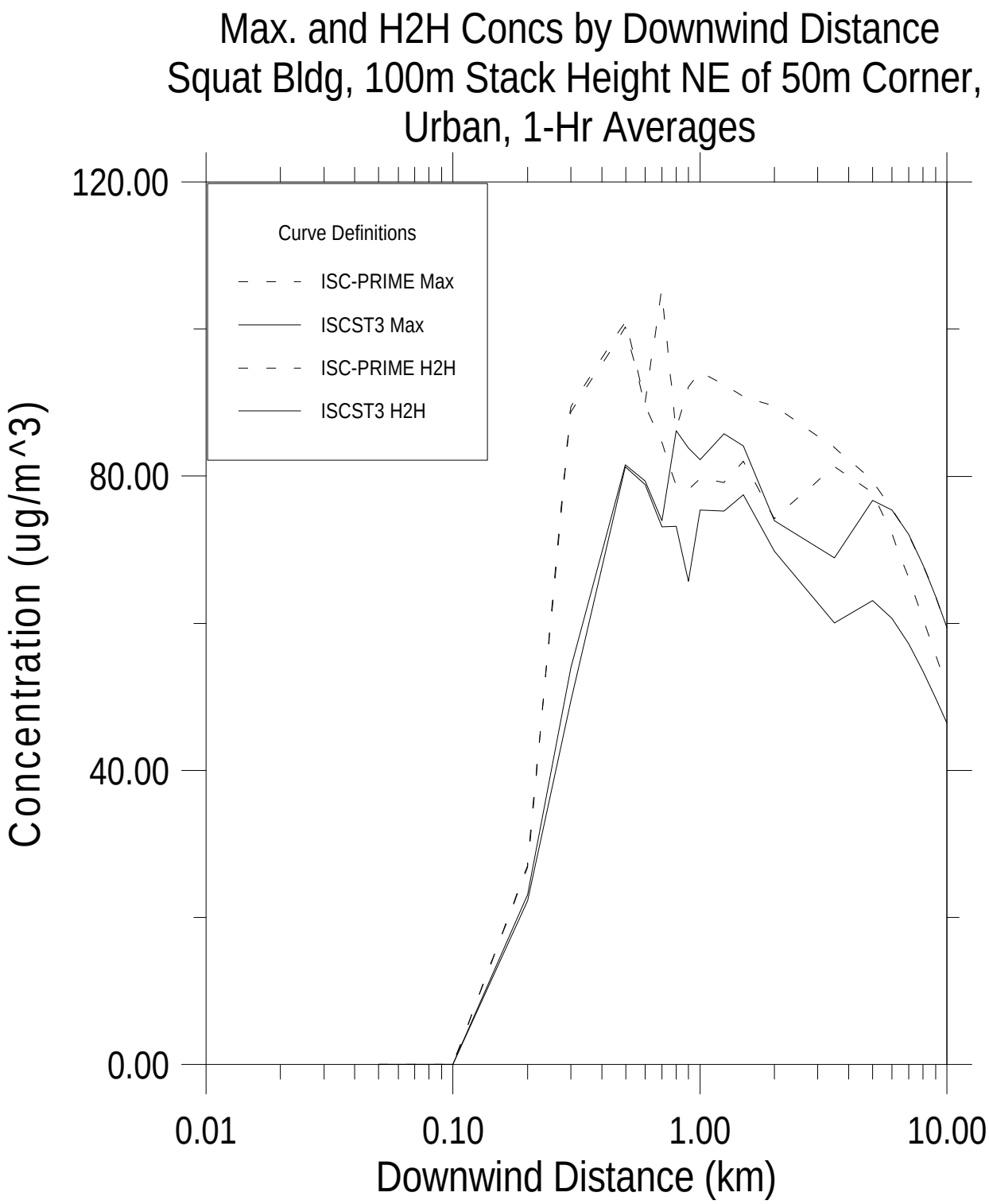

Figure 26. Maximum and Highest of the Second Highest 1-hour averaged concentrations versus downwind distance.

APPENDIX D

TABLES OF BOWLINE POINT CLOSE-IN CONCENTRATIONS

Parking Lot

Rank	Observed		
#	Conc.	Day	Hr
1	84.5	339	8
2	83.9	347	7
3	74.5	345	20
4	74.4	349	8
5	74.1	342	23
6	73.8	351	23
7	73.2	349	23
8	73.0	339	5
9	72.8	348	21
10	71.3	339	4
11	71.1	336	10
12	71.0	148	8
13	70.4	336	12
14	69.9	15	20
15	68.6	319	6
16	68.2	349	17
17	67.6	351	18
18	67.5	349	19
19	67.3	349	21
20	67.2	337	10
21	66.9	355	8
22	66.5	349	18
23	66.1	351	22
24	66.2	282	4
25	66.0	349	24
26	65.9	351	16
27	65.9	355	9
28	65.9	319	23
29	65.8	348	18
30	65.3	339	7
31	65.3	336	18
32	65.3	350	3
33	65.1	349	15
34	64.9	343	11
35	64.9	339	14
36	64.8	351	17
37	64.6	354	9
38	64.5	348	4
39	64.4	349	22
40	64.3	346	11
41	64.2	336	13
42	64.1	342	15
43	63.8	342	16
44	63.4	348	24
45	63.4	339	23
46	63.3	349	1
47	63.3	348	19
48	63.3	353	20
49	63.3	181	21
50	63.2	342	15

Parking Lot

Rank	ISCST3		
#	Conc.	Day	Hr
1	406.8	233	13
2	115.2	233	17
3	65.2	93	21
4	53.3	247	6
5	36.3	93	16
6	33.6	247	7
7	30.5	241	14
8	26.4	304	7
9	15.3	93	15
10	11.5	54	7
11	7.2	124	16
12	7.1	233	14
13	6.9	304	8
14	6.8	243	22
15	6.6	243	3
16	6.5	232	21
17	5.2	261	13
18	4.5	305	14
19	4.4	54	8
20	3.4	51	15
21	3.3	233	11
22	2.8	146	13
23	1.8	199	14
24	1.6	304	13
25	1.3	232	20
26	0.7	204	14
27	0.7	51	20
28	0.5	232	14
29	0.5	8	8
30	0.4	181	13
31	0.4	183	9
32	0.4	10	9
33	0.3	247	5
34	0.3	190	13
35	0.3	328	9
36	0.3	140	2
37	0.3	314	20
38	0.3	214	12
39	0.3	44	10
40	0.2	191	22
41	0.2	85	8
42	0.2	295	1
43	0.1	240	16
44	0.1	93	14
45	0.1	334	11
46	0.1	82	22
47	0.1	140	13
48	0.1	111	20
49	0.1	225	13
50	0.1	228	24

Parking Lot

Rank	ISC3-PRIME(2)		
#	Conc.	Day	Hr
1	185.4	93	12
2	138.2	145	14
3	127.7	221	17
4	120.5	145	13
5	117.1	145	15
6	110.4	86	20
7	101.4	89	1
8	107.8	89	2
9	107.7	93	16
10	100.0	145	18
11	99.5	93	17
12	85.9	145	17
13	91.4	93	13
14	86.4	88	23
15	73.9	88	22
16	73.8	145	12
17	73.6	227	24
18	63.0	88	21
19	59.6	100	24
20	58.2	89	6
21	54.5	99	17
22	51.1	221	19
23	50.1	202	4
24	46.9	98	1
25	44.9	145	48
26	44.0	97	20
27	44.0	74	19
28	43.6	293	20
29	42.4	88	20
30	39.0	227	23
31	37.8	202	8
32	37.2	89	21
33	36.3	74	21
34	35.3	88	3
35	35.2	221	18
36	34.8	93	24
37	33.8	200	23
38	33.4	89	10
39	33.3	160	7
40	32.3	74	16
41	31.4	97	21
42	30.9	24	10
43	28.5	227	14
44	28.2	74	18
45	27.8	221	20
46	27.5	93	15
47	26.0	89	12
48	25.9	74	20
49	25.7	227	19
50	24.1	104	16

Table 1. Bowline Point Parking Lot monitoring and associated ISCST3 and ISC-PRIME modeling data results for the top 50 1-hour average concentration values each.

Met Tower

Rank	Observed Conc.	Day	Hr
1	243.4	94	10
2	236.9	94	09
3	218.3	93	11
4	187.3	93	10
5	183.7	93	12
6	163.8	74	17
7	151.8	304	15
8	150.8	93	15
9	148.3	89	14
10	135.9	93	16
11	131.8	93	13
12	125.8	74	20
13	115.4	94	11
14	111.3	93	17
15	110.8	147	15
16	107.4	233	19
17	102.0	59	12
18	101.8	147	21
19	99.7	150	3
20	98.9	47	14
21	96.6	39	11
22	96.4	291	8
23	96.3	294	2
24	93.1	93	14
25	92.8	26	11
26	92.2	74	18
27	89.5	59	7
28	84.1	173	10
29	84.1	227	16
30	84.1	173	14
31	84.0	26	12
32	82.6	227	21
33	82.2	89	9
34	80.9	293	17
35	80.3	74	19
36	79.5	119	17
37	78.4	98	16
38	78.2	293	23
39	77.2	74	21
40	74.1	270	10
41	73.0	291	07
42	71.4	94	13
43	68.2	291	9
44	67.4	293	21
45	67.1	293	14
46	64.4	74	16
47	64.2	26	14
48	65.7	270	17
49	64.9	21	19
50	54.9	356	05

Met Tower

Rank	ISCST3 Conc.	Day	Hr
1	137.9	93	13
2	164.5	147	14
3	155.5	319	21
4	81.8	293	15
5	81.6	94	9
6	69.9	294	14
7	27.1	251	21
8	25.8	145	14
9	23.8	221	17
10	22.8	270	21
11	20.6	93	16
12	20.5	174	5
13	18.6	93	13
14	18.4	145	13
15	17.9	145	14
16	17.1	94	17
17	11.9	149	15
18	11.4	227	12
19	10.8	145	15
20	9.5	114	14
21	9.0	259	12
22	8.8	270	16
23	7.2	145	17
24	6.6	174	13
25	6.5	227	14
26	6.0	86	20
27	5.9	94	10
28	5.6	213	20
29	5.4	259	13
30	4.7	85	15
31	4.7	147	13
32	4.4	145	12
33	4.3	202	3
34	4.3	201	11
35	3.6	147	23
36	3.6	106	23
37	3.3	89	1
38	2.9	114	12
39	2.6	167	16
40	2.6	74	17
41	2.1	227	15
42	2.1	85	16
43	1.6	167	18
44	1.4	301	2
45	1.2	271	5
46	1.1	95	23
47	1.0	176	11
48	0.9	86	6
49	0.8	220	1
50	0.8	174	6

Met Tower

Rank	ISC3-PRIME[2] Conc.	Day	Hr
1	143.3	232	12
2	127.4	232	13
3	18.8	124	16
4	0.8	52	11
5	0.5	144	15
6	0.3	184	13
7	0.2	205	14
8	0.1	232	16
9	0.1	204	13
10	0.1	64	13
11	0.1	232	11
12	0.1	181	8
13	0.0	204	14
14	0.0	109	12
15	0.0	214	13
16	0.0	191	14
17	0.0	247	8
18	0.0	232	10
19	0.0	215	12
20	0.0	52	12
21	0.0	261	15
22	0.0	191	13
23	0.0	198	12
24	0.0	232	14
25	0.0	123	14
26	0.0	124	17
27	0.0	191	12
28	0.0	304	7
29	0.0	261	18
30	0.0	1	0
31	0.0	1	10
32	0.0	84	10
33	0.0	125	4
34	0.0	360	24
35	0.0	247	7
36	0.0	263	15
37	0.0	192	10
38	0.0	64	6
39	0.0	232	15
40	0.0	149	13
41	0.0	219	13
42	0.0	232	10
43	0.0	182	15
44	0.0	236	19
45	0.0	184	14
46	0.0	247	5
47	0.0	182	14
48	0.0	299	1
49	0.0	52	23
50	0.0	198	13

Table 2. Bowline Point Met Tower monitoring and associated ISCST3 and ISC-PRIME modeling data results for the top 50 1-hour average concentration values each.